Marquette University
e-Publications@Marquette

Examining Lower Extremity Motor Activity Using Magnetoencephalography

Ruth M. Swedler
Marquette University

EXAMINING LOWER EXTREMITY MOTOR ACTIVITY USING MAGNETOENCEPHALOGRAPHY

by

Ruth M. Swedler, B.S.

A Thesis submitted to the Faculty of the Graduate School,

Marquette University,

in Partial Fulfillment of the Requirements for

the Degree of Master of Science

Milwaukee, Wisconsin

August 2012

ABSTRACT
EXAMINING LOWER EXTREMITY MOTOR ACTIVITY USING
MAGNETOENCEPHALOGRAPHY

Ruth M. Swedler, B.S.

Marquette University, 2012

The role of the cortex during locomotion remains unclear, but recent advances in neural imaging technologies have aided in developing ways to measure brain activity during motor tasks. One method is by measuring activations produced by neural oscillations which have been associated with a variety of human behaviors, from sleep and rest to cognitive actions and movement. The physiological and functional methods in which oscillations contribute to cortical control are still largely unknown. In this study, we aim to expand that knowledge by examining human cortical activity in the sensory and motor cortices during pedaling using magnetoencephalography (MEG). We hypothesized that, if the sensory and motor cortices are important for controlling locomotion, then the MEG signal would differ during pedaling as compared to rest and would be modulated with the phase of the pedaling cycle. Moreover, if locomotor-related brain activity is solely caused by sensory feedback, then the MEG signal would be the same during active and passive pedaling.

We scanned eight healthy subjects using MEG while they pedaled a custom-made pedaling device. The subjects' magnetocortical activity was measured in two minute recordings during rest, continuous, self-paced active pedaling, and passive pedaling. The passive condition consisted of the subject relaxing their leg muscles while the experimenter pedaled the device for them at a velocity matching that subject's active pedaling bout. Task-dependent magnetocortical activity was examined in the primary sensorimotor cortex (M1 and S1), supplemental motor area (SMA), and premotor area (PMA).

The power spectrum of the MEG signal during the different tasks was extracted using a Welch periodogram to examine the frequency content throughout each task. The power in the alpha and beta bands of all regions of interest decreased significantly during active and passive pedaling as compared to rest. No significant difference was found between any of the tasks in the gamma band.

The temporal pattern of the beta frequency band was also examined across the pedaling cycle by performing a time-frequency decomposition using a Morlet wavelet. Both pedaling conditions demonstrated modulation of the beta band at twice the pedaling frequency. These fluctuations were not found in the rest condition.

Our results showed that the brain becomes engaged during pedaling as compared to rest. The magnetocortical activity is different across the movement cycle, suggesting that the brain has input into the regulation of locomotor-like movement. There is also a strong sensory component during movement since the active and passive pedaling conditions are similar.

ACKNOWLEDGEMENTS

Ruth M. Swedler, B.S.

TABLE OF CONTENTS

LIST OF TABLES

LIST OF FIGURES

LIST OF ABBREVIATIONS

CPG – central pattern generator

SCI – spinal cord injury

PTN – pyramidal tract neurons

EMG – electromyography

EOG – electrooculography

ECG – electrocardiography

fMRI – functional magnetic resonance imaging

NIRS – near-infrared spectroscopy

SPECT – single photon emission computed tomography

TMS – transcranial magnetic stimulation

PET – positron emission tomography

EEG – electroencephalography

MEG – magnetoencephalography

M1 – primary motor cortex

S1 – sensory motor cortex

SMA – supplemental motor area

PMA – premotor area

LFP – local field potential

HPI – head position indicator

TFD – time-frequency decompositions

wMN – weighted minimum norm

ANOVA – analysis of variance

SI – symmetry index

CHAPTER 1 - INTRODUCTION

1.1 NEURAL CONTROL OF LOCOMOTION

Walking seems like a simple task that most humans can do without thinking. However, once the task is broken down, one realizes it is a complex alternating, multi-joint process involving extension and flexion at the hip, knee, and ankle in a defined temporal pattern all while balance is maintained during forward propulsion. While kinematically complex, walking is also neurologically complex using control input from three main sections: spinal cord, sensory afferents, and supraspinal inputs.

1.1.1 THE SPINAL CORD

The spinal cord was once thought of as just a connection to relay information between the brain and the peripheral nervous system. Now it is known that the spinal column can also generate motor activity in the form of rhythmic movements and motoneuron discharge timing similar to that of normal walking. These productions by neuronal networks contained within the spinal cord are called central pattern generators (CPGs) (Marder & Calabrese 1996). It has been well known for many years that non-human animals have a CPG that allows locomotion with no supraspinal input (Grillner & Zangger 1975). Many studies have been done on spinal cats, which are cats that have been given spinal cord transections. While the data for humans is less robust, comparing to animal experiments helps in the understanding of what the spinal cord does in humans.

Cats with incomplete spinal cord lesions are able to walk on a treadmill, but with less precision than neurologically intact cats. The fore- and hindlimb coordination

becomes impaired and they lose the ability to perform skilled movements such as stepping over obstacles (Rossignol et al. 1999, Rossignol & Frigon 2011). Spinal cats with complete spinal cord lesions are also able to walk with their hindlimbs when placed on a treadmill (Barbeau & Rossignol 1987, Duysens & Van de Crommert 1998, Rossignol 2000). Intensive and repetitive training is necessary for the spinalized cats to regain that task-specific hindlimb locomotor function. While the spinalized cats express good locomotor patterns and close to normal kinematics and electromyography (EMG) activity, there are a few differences including a reduction of step length and step cycle duration as well as increased EMG amplitude of flexor muscles (Belanger et al. 1987).

Humans with incomplete spinal cord injuries (SCI) also have some remaining locomotor function (Dietz & Harkema 2004). Calancie and colleagues (1994) demonstrated that an incomplete SCI patient can produce involuntary stepping-like movements by extending the patient's hip while lying supine. The movements continue spontaneously when external perturbations are removed, suggesting that humans may also have a CPG. However, experiments involving humans with complete SCI more clearly purvey that humans do need additional sensory and perhaps supraspinal input to produce the basic walking rhythms as compared to other animals who undergo task-specific functional improvements after complete spinal cord lesions. Dimitrijevic and colleagues (1998) were able to induce locomotor-like activity (rhythmic alternating stance and swing phases of the lower limb) by constant stimulus with spinal electrical stimulation. In another study with intense, daily locomotor training similar to that of the cats, complete SCI humans do show some enhanced EMG activity suggesting functional locomotor improvement (Dietz et al. 1995). The demonstrated increase in gastrocnemius

EMG and the decrease in tibialis anterior EMG are both characteristics of muscle activity that is beneficial during stance. Ferris et al. (2004) induced stepping in the leg contralateral to the leg being rhythmically loaded, resulting in EMG similar to that seen during bilateral stepping.

While these observation show that some of the physiological activity seen in locomotion still exists after complete SCI, humans are not able to continue this activity when external perturbations and aids are removed. Thus the need exists for a greater understanding of the cortical inputs necessary for locomotion.

1.1.2 PERIPHERAL SENSORY AFFERENTS

It has been well known that reflex pathways of the peripheral nervous system can respond to an external stimulus without the signal having to go all the way up to the brain. However, research has shown that peripheral afferents also have a part in maintaining ongoing actions, such as regulating normal, unperturbed locomotor movements. Sensory input allows for corrective reflexes and adjustment of stepping patterns when unexpected terrain or perturbations arise (Pearson 1995).

Spinal cat studies have allowed for the investigation into proprioceptive feedback of extensor and flexor muscles during walking. The studies examining the extensor muscles give insight into the stance phase and the stance-to-swing transition. Duysens and Pearson (1980) showed that unloading of the ankle extensors at end of stance allowed for swing to begin. The angle of extension of the hip is also important for the initiation of swing. When spinal cats performed hind limb treadmill walking and one limb was held and slowly pulled back by experimenters, that limb snapped forward into the swing

phase once it reached a certain extension angle (Grillner & Rossignol 1978). The stimulation of extensor muscle nerves during stance and swing showed, respectively, a delayed onset of the flexor burst activity that starts the swing phase (Guertin et al. 1995) and a sudden stop of flexion with a reset of the gait cycle to the stance phase (Whelan et al. 1995). Studies on flexor muscle proprioceptive feedback have shown analogous functions to extensor feedback. Hiebert et al. (1996) showed that feedback of stretch-sensitive afferents in flexors during stance reset the locomotor rhythm, while also inhibiting extensor activity to allow swing to start. Specifically, the hip flexors of decerebrate cats have modulated activity during locomotion by modifying proprioceptive feedback from those muscles (Lam & Pearson 2001).

Similar to animal studies, experiments on humans suggest peripheral afferents influence locomotion by regulating the timing, amplitude, and modulation of the gait cycle.

Reflex modulation occurs in humans during walking when muscle reflexes, such as stretch and load receptor, aid in force production and body weight support during stance, stabilization of limb trajectory, and step cycle timing (Stephens & Yang 1996a, Zehr & Stein 1999). The quadriceps H-reflex, an extensor reflex, has a higher amplitude during stance than swing (Dietz et al. 1990) while Brown and Kukulka (1993) showed the amplitude, pattern and onset latency of human flexor reflex pathway in the tibialis anterior and soleus muscles also undergo phase-dependent modulation. This shows both extensor and flexor reflex pathways regulate the timing of stance-to-swing transition and control magnitude of ongoing motoneuronal activity (Pearson 1995).

The regulation due to proprioceptive signals is similar to what is seen in animals.

Increased or decreased loading of the leg during stance phase of healthy humans

increased the extensor EMG activity.   In adults, the step cycle duration was not affected

by the loading (Stephens & Yang 1999), while the step cycle of infants was indeed

prolonged (Yang et al. 1998), suggesting stepping adaptations are in humans from birth.

In human SCI, i.e. no supraspinal input, electrical stimulation over the hip flexors

affected the timing of muscle activity during walking, which is consistent with animal

studies (Wu et al. 2011).

Inhibition signals from peripheral afferents also influence the modulation

occurring in walking. Iles et al. (1996) showed that Ia afferent presynaptic inhibition is

modulated in the lower limb and is controlled by both peripheral nerves and corticospinal

input. Group I inhibition in the extensor muscles that is usually found during rest in

humans is reduced during walking, specifically throughout the stance phase (Stephens &

Yang 1996b, Faist et al. 1996).

1.1.3 SUPRASPINAL INPUT

The third, and least understood, factor to locomotor neural control in humans is

supraspinal input. There are a few reasons this component's contribution has been the

least studied. For one, there were many years when research was focused on the central

pattern generators, which alone could produce locomotor movements in animals. When

it was discovered that humans need more supraspinal input to produce basic walking

patterns (Nielsen 2003), a new issue arose. Researchers now had the difficult task of

measuring activity of the cortex and deeper brain structures in humans. Experiments in

this field once again began with animal models allowing for direct recording of motor

cortical cells and decerebration, but recording human cortical activity through the skull proved challenging.

It has been shown in cats that the brain contributes to the initiation and regulation of locomotion. Shik et al. (1966) applied a tonic electrical stimulation to the mid-brain of decerebrate cats to initiate stepping as well as increase the speed of walking when the intensity of the stimulation was increased. However, cortical input is particularly necessary when a disruption occurs and the normal gait must be modified (Drew et al. 2002). Obstacles placed on a treadmill have been used to cause a modification of gait in cats. As healthy cats approach an obstacle, three things happen: their limb trajectory changes, forelimb flexor activity increases, and the discharge of pyramidal tract neurons (PTNs) increases (Drew 1988). The increase in PTN discharge, as well as the modulation of discharge based on timing of the step cycle (Drew 1993), suggests a cortical control in gait modification. Studies in which the motor cortex had been lesioned or inactivated, cats were not able to adjust their limb trajectory to step over obstacles (Drew et al. 1996).

Similar to the animal studies, it has been shown that humans use the descending pathways from the cortex and brain stem for the initiation and control of walking. Miyai et al. (2001) measured brain activity based on hemoglobin levels using near-infrared spectroscopy (NIRS) while subjects walked on a treadmill. An increase in cerebral activity was seen bilaterally in the medial primary motor area (M1), primary sensory cortex (S1), and supplemental motor area (SMA) during walking as compared to alternating foot movements. Fukuyama et al. (1997) found the same areas of activation during walking using single photon emission computed tomography (SPECT). Studies utilizing transcranial magnetic stimulation (TMS) are also useful in demonstrating the

contribution of the corticospinal tract in walking. Strong TMS signals applied on the motor cortex has shown increased muscle activity during walking (Petersen et al. 1998, Schubert et al. 1997, Capaday et al. 1999) as well as a modulation of motor evoked potential amplitudes in a phase-dependent manner across the gait cycle (Schubert et al. 1997). On the other hand, Petersen and colleagues (2001) also showed that weak magnetic stimulation with TMS causes suppression on EMG activity. This shows that when inhibition occurs with a low TMS stimulus causing the cortical input to be removed, the muscle activity is affected. Thus, the corticospinal tract has a direct effect on uncomplicated motor tasks.

Unfortunately, the physical constraints of neural imaging modalities have restricted the amount of research done during walking. Thus, scientists have resorted to other gait-like tasks and movements to piece together more information on the supraspinal input of locomotion. A simple stationary task examining lower extremity movement would be ankle flexion and extension. Studies in functional magnetic resonance imaging (fMRI) (Miyai et al. 2001, Sahyoun et al. 2004, Ciccarelli et al. 2005) and near infrared spectroscopy (NIRS) (Miyai et al. 2001) show bilateral activation of the medial primary sensorimotor regions and supplementary motor regions during ankle movements. During pedaling, the same areas along with the cerebellum were activated in positron emission tomography (PET) (Christensen et al. 2001) and fMRI (Mehta et al. 2012). TMS during pedaling, as shown by Sidhu et al. (2012), resulted in phase-dependent EMG modulation across the cycle, much like what was seen during walking.

A concern with movement studies becomes apparent when trying to decipher the activation relating to the sensory signals being sent back up to the brain and the signals

the brain sends to produce movements. Imaging the brain during passive movements helps give insight into the sensory aspect of movement production. Christensen et al. (2000) and Mehta et al. (2012) used PET and fMRI, respectively, during passive pedaling and saw that the same areas were activated during active and passive pedaling with not much difference in activation levels. Electroencephalography (EEG) waveforms across the pedaling cycle had larger amplitude in passive than active pedaling (Gourab et al., in review). However, comparing passive and active ankle movements in fMRI, Sahyoun and colleagues (2004) showed a lower activation level during passive movements. It can be said that passive movements activate similar areas during the brain as the comparable active movements, but it is still unknown how the level of activation is involved.

1.2 NEURAL OSCILLATIONS

Neural oscillations became an intriguing topic in neuroscience after it was first noticed with EEG recordings that the signal power modulated at different frequencies depending on a task, or lack of task, that a human performed (Berger 1929). In the past two decades there has been much interest in studying the synchrony of oscillations and the functional significance they are thought to have. As mentioned, neural oscillations can be measured with EEG, but also magnetoencephalography (MEG) as well. These are the two forms of recordings used due to the necessity of a high temporal resolution for the frequency bands to become apparent.

1.2.1 PHYSIOLOGICAL BACKGROUND

Neural oscillations do not refer to a single neuron firing at a given frequency. Rather, the firing patterns of a population of neurons are reflected in the local field potential (LFP). The LFPs are a summation of the voltage fluctuations from information transmission in the form of excitatory and inhibitory post-synaptic potentials (Bennett & Zukin 2004). If many neurons in a local population fire in similar patterns then these patterns are enhanced in the sum. These consistent neuronal firings are thought to be a form of communication between areas of the brain. Communication between areas can be thought of in two ways: either one area is driving the other or one area is modulating the drive of the other (Schnitzler & Gross 2005). The exact method in which the brain functionally utilizes neural oscillations as a form of communication is still largely unknown. One theory is that neuronal projections connecting the thalamus and cortex are the basis of the oscillations (Steriade et al. 1993).

The frequency bands of the human cortex are as follows: delta (< 4Hz), theta (4-8Hz), alpha (8-12Hz), beta (13-35Hz), gamma (>35Hz). The lower bands, delta and theta, are related to sleep, drowsiness, and other idling-like activities. The higher frequency bands tend to have a functional relation concerning various activities, as will be discussed later in more detail relating to motor activity.

When populations of neurons fire together, the rhythmic pattern is termed synchronization. While it seems contradictory, the synchronized firings are caused by decreased excitability of the cortex and are correlated with an increased power. The synchronization of neural oscillations can be thought of as an idling state in which the brain is ready to trigger a particular functional pathway (Steriade et al. 1993). On the

other hand, a drop in power in a frequency band is called desynchronization and is related to cortical activation during a task. Desynchronization has been correlated to increased excitability in the thalamacortical systems (Steriade & Llinas 1988).

1.2.2 FREQUENCY BANDS IMPORTANT IN MOVEMENT

The most studied and documented frequency bands relating to movement are the alpha and beta bands. Also commonly referred to in motor control as the 10- and 20-Hz rhythms, respectively, the alpha and beta bands desynchronize (decrease power) during a movement and synchronize (increase power) up to baseline levels following the movement (Conway et al. 1995, Salmelin et al. 1995, Pfurtscheller 1997). In support of this theory, Chen and colleagues (1999) applied TMS to the motor cortex at different intervals following median nerve stimulation to examine how cortical excitability corresponds to the synchronization after stimulation. They found inhibition in the cortex, supporting the hypothesis that increased power, or synchronization, does indeed represent decreased cortical excitability.

Throughout the MEG and EEG studies examining the power spectra of various movement tasks [low-level isometric finger contractions (Conway et al. 1995), discreet finger and toe movements (Alegre et al. 2004, Pfurtscheller et al. 1997), simple repetitive finger and toe movements (Salmelin et al. 1995, Erbil & Ungan 2007), difficult bimanual learning task (Boonstra et al. 2007), continuous lower extremity movements (stepping, Raethjen et al. 2008; pedaling, Gourab et al., in review; walking, Gwin et al. 2011)], the common finding has been a task-dependent desynchronization of the alpha and beta bands. Larger decreases in the beta band were seen with increasing difficulty of

movements (Boonstra et al. 2007, Gross et al. 2005). When Salmelin and colleagues (1995) examined the 10- and 20-Hz rhythms during finger, toe, and mouth movements, they noticed a difference in the spatial localizations of the two rhythms. The 20-Hz rhythm showed activity in the contralateral hand, toe, and mouth area respective to the movement performed, but the 10-Hz rhythm showed bilateral activation in the hand areas regardless of the type of movement. Conversely, Pfurtscheller et al. (1997) showed an overall synchronization, or cortical deactivation, in the hand area during the toe movement.

In more recent years, the activity of the gamma band has been thought to have an important role in motor control. However, gamma oscillations react oppositely of how alpha and beta oscillations generally do in comparable movement tasks. Huo et al. (2010) showed that the contralateral motor cortex underwent a synchronization of gamma activity while the ipsilateral motor cortex was desynchronized during the simple finger movements. The MEG recordings of Conway et al. (1995) had a distinct 40-50 Hz peak during rest which was then enhanced during low-level isometric finger contractions. Gwin et al. (2011) also showed an increase of gamma power during walking.

With several techniques available in functional neuroimaging, it is important that the measured variables give practical information about how the brain functions. Studying cortical activations as measured by neural oscillations gives insight into how the brain communicates within itself. This information covers the whole spectrum of human behaviors, from sleep and rest to cognitive actions and movement. It has also been noted that certain pathologies can lead to abnormal synchronization patterns (Schnitzler & Gross 2005). This suggests the possibility of using neural oscillations as biological

markers to help diagnose disorders. For example, movement disorders such as Parkinson's are associated with synchronization patterns between the basal ganglia and cortical structures that are different than normal motor behaviors (Hutchinson et al. 2004).

1.2.3 MEG BACKGROUND

MEG is a functional imaging technique that passively measures the changing magnetic field in the brain. It stems from the electrophysiology field, which began in the 1920s when Hans Berger first recorded the brain's electrical activity. The source of MEG signal are the neural currents. The magnetic fields produced by the brain are magnitudes smaller than other physiological activity, thus very sensitive sensors, called SQUIDs (superconducting quantum interference devices), must be used. SQUIDs act at very low temperatures (4 K) and are kept cold with liquid helium. MEG recordings must be done within a magnetically shielded room to prevent environmental noise artifacts from distorting the magnetic signal (Hamalainen et al. 1993). The main clinical use of MEG is as a non-invasive pre-surgical planning tool for epilepsy surgery. The topics of research on MEG range between cognitive processes, language, visual systems, and movement (Hari and Salmelin 2012).

MEG has recordings similar to those captured with EEG due to the fact that the magnetic fields stem from the electrical current flowing throughout the brain and the high temporal resolution with which they both record. However, magnetic fields are much less distorted by the layers of tissue and bone between the sources and sensors than

electrical currents. This produces a better spatial resolution in MEG (3 mm) as compared to EEG (2 cm) (Matre 2009).

This imaging technique will be helpful for our application since it allows for underlying neural oscillations to be studied during continuous motor tasks. Previous lower extremity, continuous movement studies have used frequency analysis of EEG recordings to examine rhythmic neural activity in stepping (Raethjen et al. 2008), pedaling (Gourab et al., in review), and walking (Gwin et al. 2011). While these experiments give insight into the frequency analysis of movement, utilizing MEG will give a more precise depiction of location of neural activity.

1.3 EXPERIMENTAL OVERVIEW

The role of cerebral cortex in controlling locomotion is still unclear. With the use of past research findings and our own experimental results, we aim to enhance our understanding of cortical control of locomotion using frequency analysis. In this study we used MEG to examine human brain activity in the sensory and motor cortices during pedaling. The benefit of using MEG rather than other functional imaging techniques with similar high spatial resolution, such as fMRI, is the high temporal resolution. MEG records up to millisecond resolution, allowing changes in neural activity to be examined throughout different phases of a movement.

Similar to the constraints of many functional imaging devices, walking is not possible in a MEG scanner. Therefore, we aim to study locomotor brain activity using pedaling in order to have minimal head and body displacement. While pedaling is not the same as walking in that balance is not required and body weight support is not involved,

it does have similar characteristics to walking and can thus be used as a model of locomotion. Another benefit of pedaling is it allows us to test a passive condition, which cannot be examined during walking.

1.3.1 HYPOTHESIS

Past studies suggest the brain is involved in the control of locomotion. We hypothesized that the sensory and motor cortices are important for controlling locomotion, thus the MEG signal would differ during pedaling as compared to rest and would be modulated with the phase of the pedaling cycle. Moreover, locomotor-related brain activity is solely caused by sensory feedback, thus the MEG signal would be the same during active and passive pedaling.

CHAPTER 2 - METHODS

In this experiment, we used MEG to examine brain activity associated with pedaling. Eight healthy, right-handed individuals (4 females, mean age of 27 years, range 22-34) participated voluntarily. All participants were free of neurological impairments and were able pedal for 15-20 minutes against a light load while lying supine on a scanner bed. No participants had metal implants or devices that would cause artifacts on the MEG signal; nor did they have contraindications for MRI such as pregnancy, claustrophobia, or obesity. Each participant gave written informed consent in accordance with institutional guidelines at Marquette University and the Medical College of Wisconsin and in accordance with the Declaration of Helsinki.

2.1 INSTRUMENTS

The pedaling device used for this study was described in a previous publication (Mehta et al., 2009). In short, it was a direct drive apparatus fabricated from nonmetallic materials that could be positioned on a MEG scanner bed. See Figure 1. The device was equipped with a custom designed non-metallic optical encoder (model TD 5207, Micronor Inc., CA) that was coupled to the crank shaft and used to measure crank position to a resolution 1.8˚. Signals from the encoder were output via a fiber optic cable to a controller unit (model MR 310, Micronor Inc., CA) located outside the scanner room. The controller unit converted the optical signals to electrical signals and produced analog outputs corresponding to position. Position data were sampled at 2000 Hz using a desktop computer, a 16 bit analog to digital converter and Elekta Neuromag® data

acquisition software. These data were used to identify the position of the crank across the pedaling cycle and to compute mean pedaling velocity within pedaling trials.

MEG scanning was performed on an Elekta Vectorview instrument containing 306 MEG channels (204 planar gradiometers and 102 magnetometers.) Magnetic shielding of the scanner was provided by a 7 ton magnetic shielded room with active flux compensation with MaxShield technology (Elekta, Sweden). Electomagnetic receiver
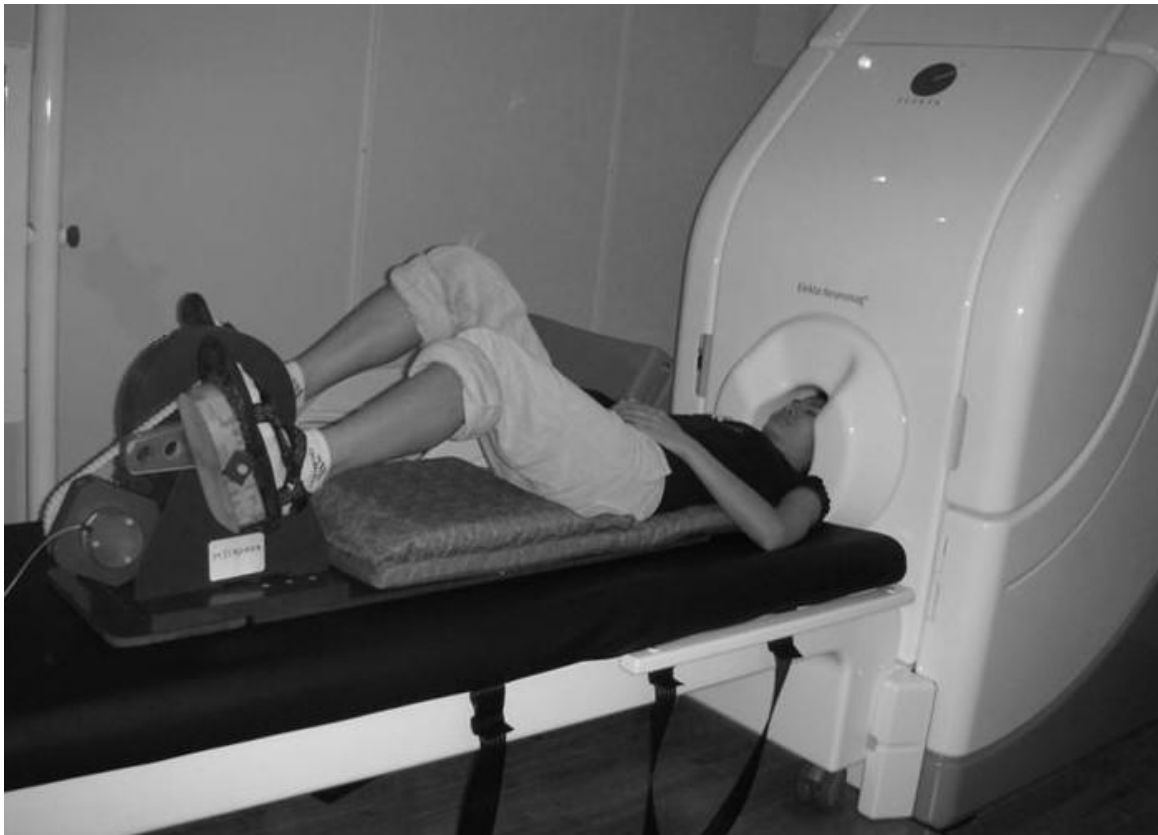
Figure 1. Custom pedaling apparatus on the MEG scanner bed.

coils were utilized as the head position indicators (HPI) (3-D Fastrak digitizer, Polhemus, Inc, USA). Electrooculogram (EOG) and electrocardiogram (ECG) data were collected using single-use, self-adhesive surface electrodes (Neuroline 720, Ambu, Denmark). These data were also sampled in Elekta Neuromag® via the analog to digital converter (Elekta, Sweden) at a rate of 2000 Hz. Anatomic images of the brain were obtained using

a 3.0 T MR scanner (General Electric Healthcare, Milwaukee, WI) and an 8-channel high

resolution brain radio frequency coil.

2.2 EXPERIMENTAL PROTOCOL

Prior to the MEG scan, subjects were screened for MEG compatibility and asked

to remove any external metal such as jewelry or clothing that would interfere with the

magnetic signal. After explaining the experimental tasks, HPI coils were placed on the

left and right aspect of the forehead and over each mastoid process. The location of the

HPI coils, the left and right preauricular points, and the nasion were localized into 3D

space for future MEG/MRI coregistration. EOG electrodes were placed on the supra- and

infra-orbital foramen of one eye. ECG electrodes were placed on the right clavicle and

lower left ribs. A common reference electrode was placed over the right scapula. EOG

and ECG signals were used for artifact removal.

Before subjects entered the shielded room, an empty room recording was taken

which was later used to calculate the noise covariance matrix to remove the

environmental noise from the MEG recordings.

Subjects entered the magnetically shielded room and lay supine with their head

placed in the dewar and both feet secured to the pedals (Figure 1). After individuals were

made comfortable, MEG scans were performed during three different conditions: rest,

active pedaling, and passive pedaling. During the rest condition, subjects were asked to

relax and lay still for 2 minutes. During active pedaling, subjects were asked to pedal

continuously at a constant, self-selected velocity for 2 minutes. During the passive

condition, individuals were instructed to relax their leg muscles as much as possible

while the experimenter pedaled the device for the subject for 2 minutes at the same

pedaling velocity that the subject had self-selected during active pedaling. The

experimenter was given an audio cue via earphones to maintain the desired velocity.

On a separate day, individuals returned for an MR anatomical scan of the brain.

After screening for MRI safety, the subject entered the scan room and lay supine on the

MR scan bed with their head positioned in the RF coil. Scanner parameters were as

follows: TE = 3.0 ms, TR = 7.8 ms, flip angle = 12°, FOV= 24 mm, matrix of 256×224,

and slice thickness of 1 mm.

2.3 DATA PROCESSING AND ANALYSIS

Preprocessing of MEG data consisted of filtering environmental noise that passed

through the magnetic shielding using signal space separation by MaxFilter (Elekta,

Sweden). This was done by relating the noise covariance matrix recorded before the

subject entered the scanner room with the source space surrounding the subject's head.

Thus, the far-field environmental noise is removed from the sources in the recordings

(Taulu et al. 2004). Electrophysiological signals from the heart and eye were minimized

using principal component analysis in MNE software (Athinoula A. Martinos Center at

the Massachusetts General Hospital, Harvard Medical School). The first and second

components of the EOG and ECG signals were removed from the MEG sensor

recordings. The MEG data were then divided into epochs that were two consecutive

pedaling cycles in length and overlapped each cycle. The top-dead-center position,

which was the point in the cycle were the left foot was closest to the hip, defined the

starting and ending position of a cycle. Epochs were spline interpolated to 2000 points

after which they were imported into Brainstorm (Tadel et al. 2011) for further analysis. Since the resting data did not have cycles to be divided into, epochs were defined using the event file of that subject's active pedaling condition. Thus the resting data were comparably split into epochs to be further analyzed. Anatomical images of the cortical brain surface were also imported into Brainstorm after segmentation from the MRI volume using the automated image-analysis pipeline of brainVISA (http://brainvisa.info).

Distributed source modeling of MEG traces was used to estimate the cortical origins of task-dependent neural activity. First, an individual head model for MEG was obtained using the overlapping-spheres approach (Huang et al. 1999) as implemented in Brainstorm (Tadel et al. 2011). A weighted minimum-norm (wMN) model of cortical currents (Baillet et al. 2001), also as implemented in Brainstorm, was obtained to determine sources after co-registration of the individual T1-weighted MRI volume to the MEG coordinate system.

Changes in the frequency content of the MEG signal were examined in 4 regions of interest: primary motor cortex (M1), primary sensory cortex (S1), premotor area (PMA), and supplemental motor area (SMA). The regions were chosen due to previous motor activity literature and preliminary source localizations of the raw MEG signal (Figure 2). These regions were defined on the standardized MNI/Colin27 brain (Holmes et al. 1998) as Brodmann's areas 4 (M1), 312 (S1), and the lateral (PMA) and medial (SMA) aspect of area 6. In each of these regions and for each condition, a power spectrum was calculated and a time-frequency decomposition was performed.

The power spectral density was calculated with a Welch periodogram across the subject's entire recording in the source domain for each condition. A Hanning window

with a length of 2000 and 50% overlap was used. The spectra were then averaged across

subjects.
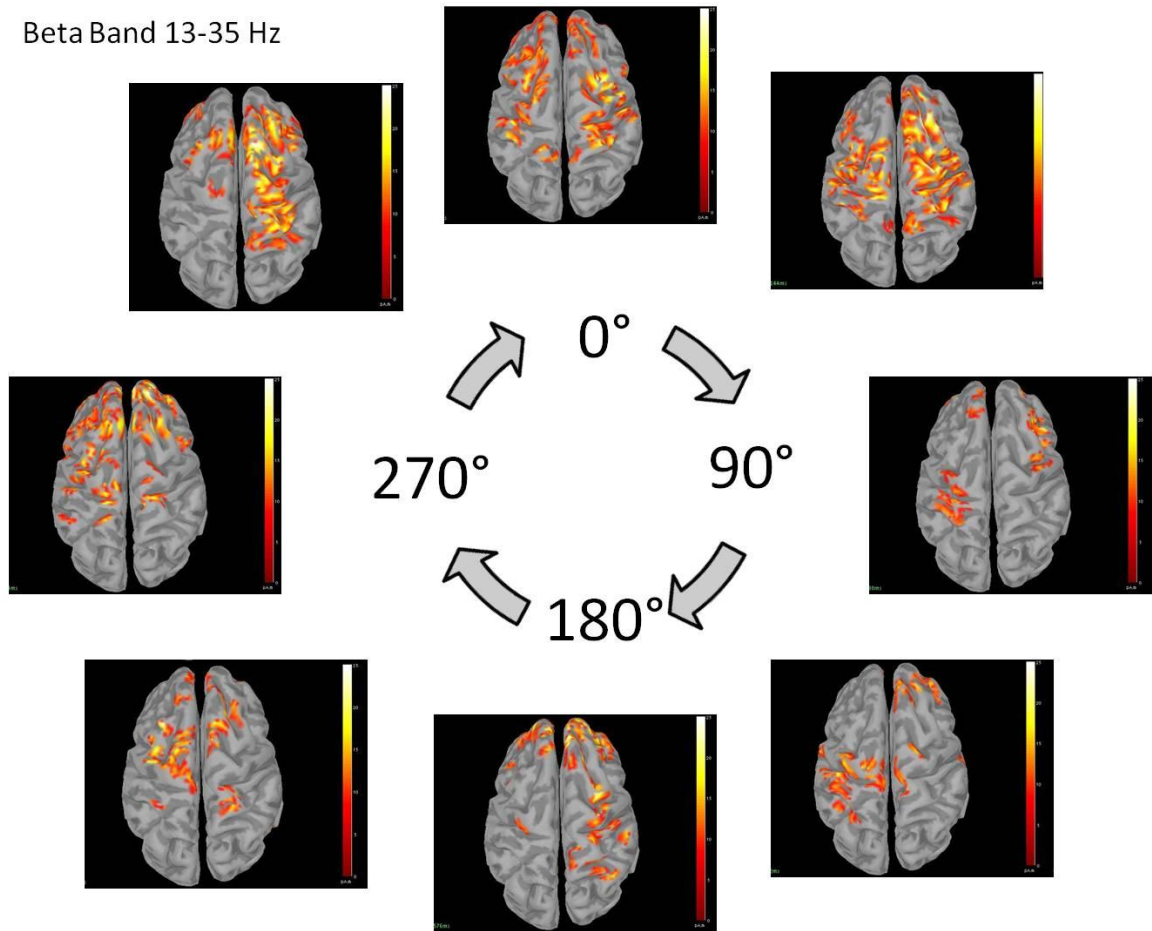
Figure 2. Single subject localizations throughout the pedaling cycle. Data was filtered from 13-35 Hz for beta band activity visualization.

The dependent variable statistically examined was the mean power of the

magnetic signal. The global effect of the mean power was examined using a univariate 3-

way ANOVA with frequency bands, pedaling conditions, and regions of interest as

factors. There was low variability from the brain areas (P=0.198) or between

hemispheres (P=0.166) allowing all eight regions of interest to be combined for statistics

to be performed. One-way ANOVAs were done to determine simple effects on each

frequency band. Tukey post hocs were then calculated on the frequency bands that

showed significant simple effects to determine differences between pedaling conditions.

Time-frequency analysis was used in order to examine modulation of frequency content across time in each region of interest. The time-frequency decomposition (TFD) was calculated for each region of interest on the divided epochs using wavelet analysis. The time signal is convolved with the Gaussian window of a Morlet wavelet (temporal resolution 3 seconds, central frequency 1Hz) to produce a spectrogram of the MEG signal power at each frequency within an epoch (Tallon-Baudry & Bertrand 1999). Data were averaged across time to produce a mean spectrogram for each subject. Mean data were z-score normalized with respect to the pedaling cycle and averaged across subjects. Averaged envelopes were computed from the group decomposition for the beta band (13-35 Hz) to better illustrate beta power fluctuations across the pedaling cycle. The envelopes were calculated by averaging the z-score values from 13-35 Hz at each time point across the cycle. For visualization purposes, a 2nd order Butterworth low-pass filter with a cutoff frequency of 5Hz was used on the envelopes before averaging across subjects. We solely looked at the beta band for the TFD results due to the poor resolution of wavelet calculations in high and low frequencies. The envelopes were quantified by calculating peak-to-peak values for the amplitudes of each hemisphere's curve per condition.

To examine the difference of modulation amplitude between pedaling cycle phases, we extracted the peak z-score values from the first half and second half of each subject's averaged envelopes. For the active and passive pedaling trials, we organized the cycle halves into flexion and extension categories, with the assumption that each hemisphere is used to co

ntrol the contralateral leg, as depicted in Figure 3. The rest trial peak values

remained labeled as first and second half since no movement occurred in those trials.

The dependent variable used in statistical analysis was referred to as the symmetry index,

which represented the difference between the flexion and extension peak z-score values.

A 3-way ANOVA among the regions of interest, hemispheres, and conditions was

performed. No effect of region of interest was found (P=0.749) thus the analysis could

be collapsed across regions. A t-test was performed on the rest condition to determine no

statistical significant difference from zero (P=0.577). The rest condition was then used as

a baseline representing no modulation across time during a one-way ANOVA with a
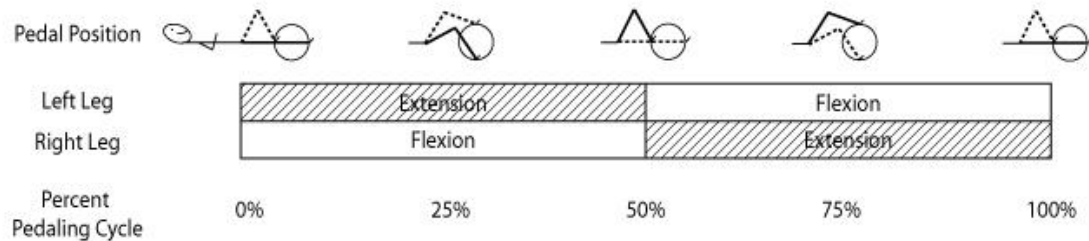
Tukey post hoc comparing conditions.

Figure 3. The positioning of the legs during each part of the pedaling cycle, starting with the left leg closest to the subject's body, also known as top-dead-center (TDC). Left Leg – dotted line, Right Leg – solid line.

CHAPTER 3 - RESULTS

3.1 EFFECT OF CONDITION ON MEAN POWER IN ALPHA, BETA, AND GAMMA BANDS

In the alpha and beta bands, the mean power of cortical activity measured by MEG decreased significantly during pedaling as compared to rest. Decreased power in these frequency bands occurred during both active and passive pedaling (Figure 4a-d) and was evident in all four regions of interest examined. There was no pedaling-related change in the power of the gamma band in any region examined. A summary of mean power values for each frequency band, condition, and region of interest can be found in Table 1.

These observations were supported statistically by a significant frequency by condition interaction (P=0.040) and by significant simple effects of condition at the alpha and beta frequencies (P<0.001 for both alpha and beta) but not at the gamma frequency (P=0.052). See Figure 4e. Post hoc analysis on the alpha and beta frequencies revealed that the power during active and passive pedaling was significantly lower than rest (P≤0.001) in both frequency bands, but there was no significant difference in power between active and passive pedaling (P=0.957 alpha, P=0.842 beta).
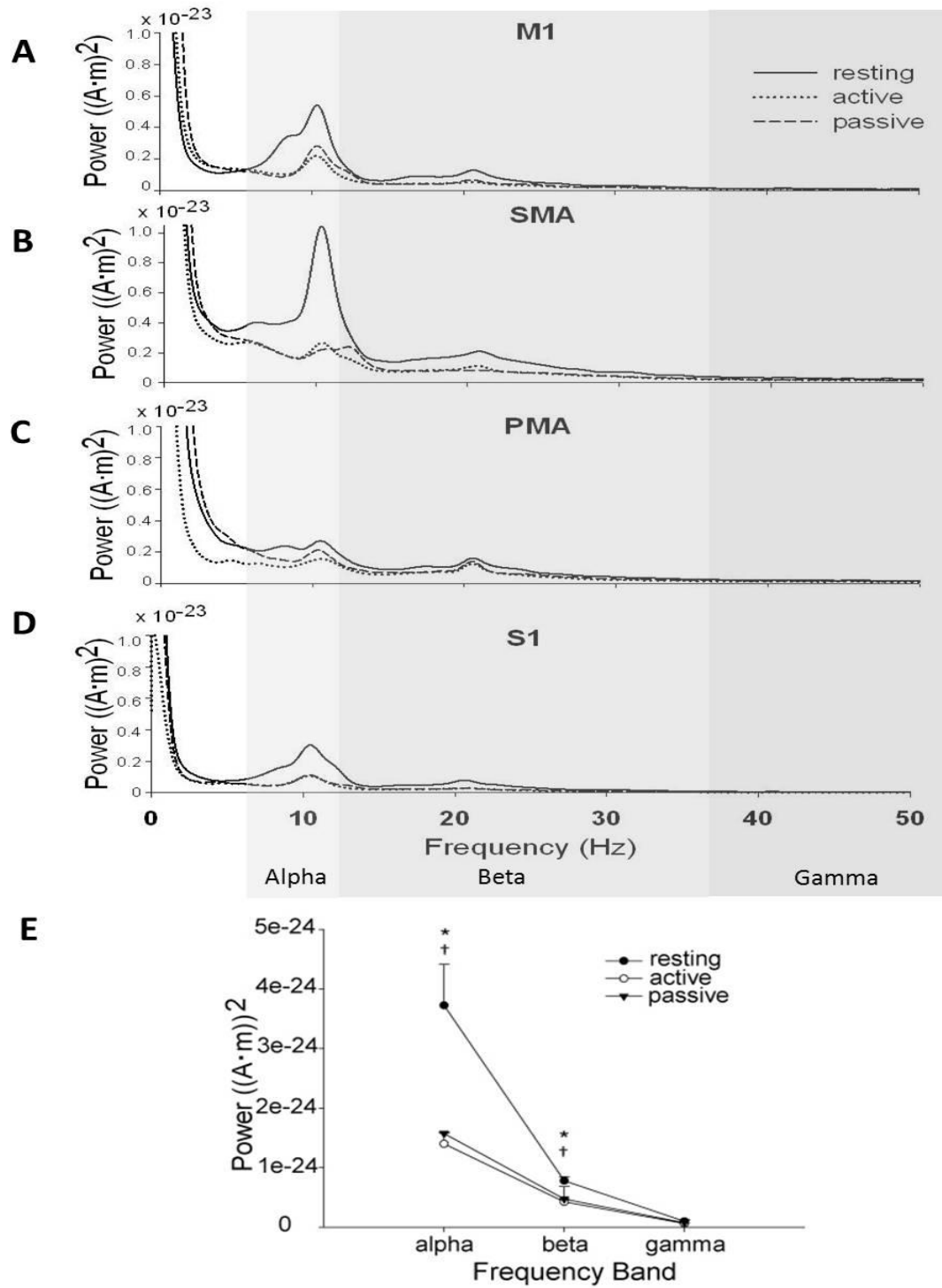
Figure 4. The power spectra for 0-50 Hz in (A) M1, (B) SMA, (C) PMA, and (D) S1 during rest and each pedaling condition. Frequency bands of interest denoted by gray shadings: alpha (8-12 Hz), beta (13-35 Hz), and gamma (>35 Hz). (E) With a significant frequency band by condition interaction (P = 0.040), Tukey post hoc analysis was used on the alpha and beta bands to determine significantly lower power during active (*, $P \leq 0.001$) and passive (†, $P \leq 0.001$) pedaling compared to rest. No significant differences between active and passive pedaling conditions in any frequency bands. Error bars are standard error.

Table 1. Averaged power spectra values across alpha, beta, and gamma frequency bands for each condition and region of interest. Values are mean(standard error) with units of $x10^{-24}$ $(A \cdot m)^2$.

	alpha (8-12 Hz)			beta (13-35 Hz)			gamma (>35 Hz)		
	rest	active	passive	rest	active	passive	rest	active	passive
M1	3.82(1.16)	1.50(0.38)	1.79(0.48)	0.63(0.06)	0.34(0.05)	0.38(0.04)	0.05(0.01)	0.04(0.01)	0.04(0.01)
SMA	6.54(2.31)	2.03(0.49)	2.06(0.33)	1.28(0.16)	0.67(0.10)	0.72(0.08)	0.17(0.03)	0.10(0.01)	0.11(0.02)
PMA	2.34(0.38)	1.30(0.43)	1.66(0.54)	0.81(0.13)	0.52(0.15)	0.60(0.18)	0.14(0.02)	0.09(0.02)	0.13(0.05)
S1	2.20(0.57)	0.76(0.21)	0.78(0.19)	0.41(0.07)	0.17(0.03)	0.20(0.04)	0.03(0.01)	0.02(0.01)	0.02(0.01)

3.2 MODULATION OF BETA BAND POWER DURING PEDALING

As shown in Figure 5, the power of brain activity in the beta band was modulated across the pedaling cycle in all regions of interest. During active and passive pedaling, fluctuations in beta power were observed at approximately twice the pedaling frequency in all regions of interest. These fluctuations in beta power were likely related to the pedaling task, as similar fluctuations were not apparent during rest. These observations are visually apparent in the group averages in Figures 5 and 6, which show the envelopes of the normalized TFDs averaged across all frequencies in the beta band collapsed across regions (Figure 6) and separately in each region of interest (Figure 7).

Indeed, the peak-to-peak amplitudes of the averaged envelopes express the differences in depth of modulation between conditions. See Table 2. Both hemispheres in rest had lower peak-to-peak values than active pedaling, which is turn was lower than passive pedaling.
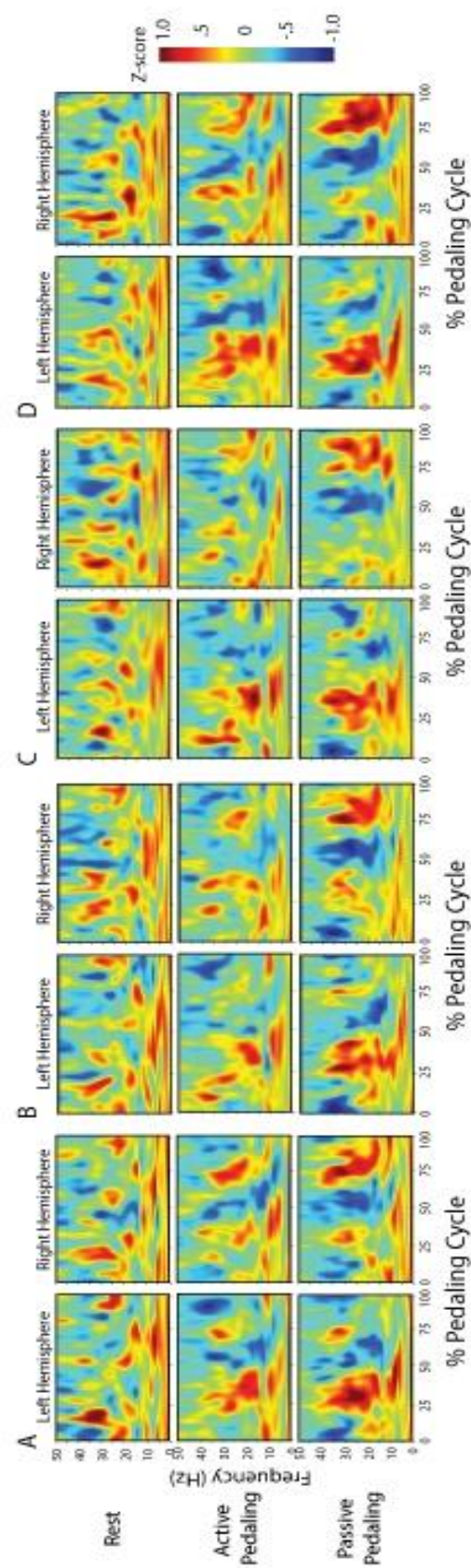
Figure 5. Group mean z-scored time-frequency decompositions across the pedaling cycle for each region of interest (A-M1, B-SMA, C-PMA, D-S1), hemisphere, and condition. Hot colors represent power at a given frequency that is higher than the mean power for that frequency. Cool colors represent lower than mean power values. Note the large splotches of blue and red throughout the cycle during passive and active pedaling. These large areas suggest a patterened modulation across time.
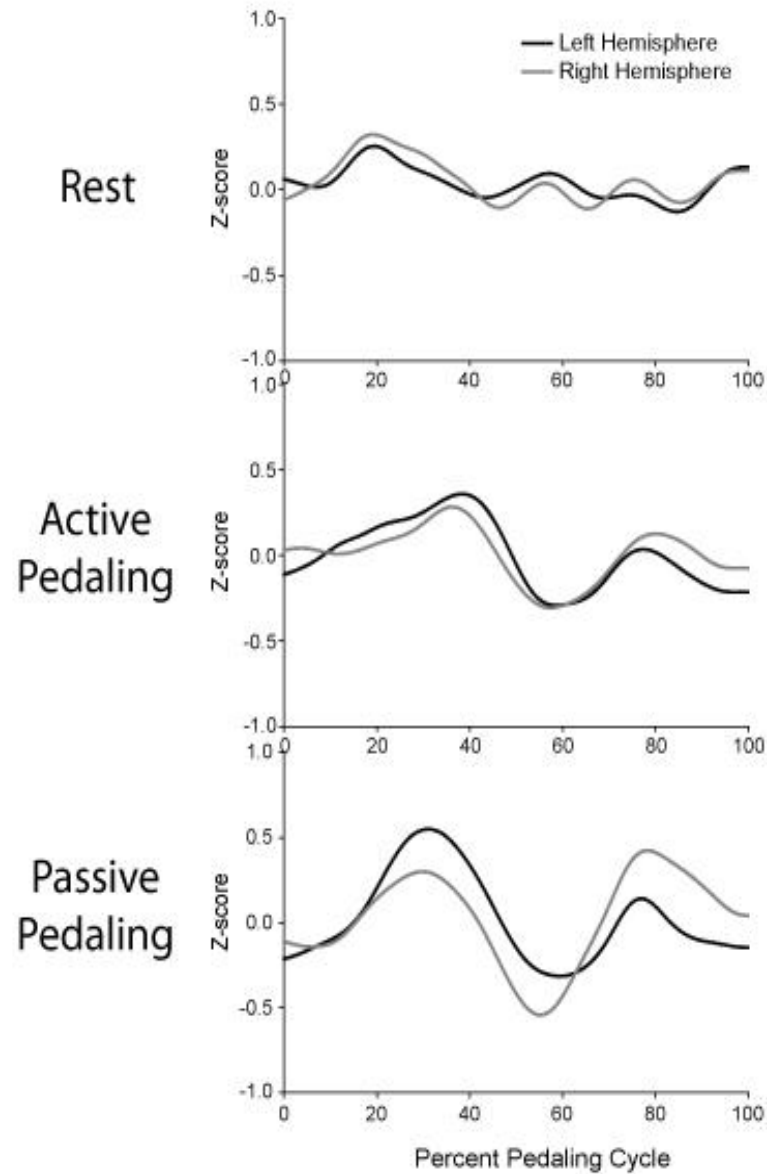
Figure 6. Group averaged z-score envelopes across the beta band (13-35 Hz) of the TFDs. No significance was found between the four regions of interest, thus averaged across areas for each condition.

Table 2. Peak-to-peak values of averaged envelopes demonstrating the deeper modulation of the pedaling conditions as compared to rest.

	Left Hemisphere	Right Hemisphere
Rest	0.36	0.41
Active	0.67	0.57
Passive	0.81	0.96

Figure 7. The z-scored envelopes split into the four regions of interest. Aids in depicting the beta band fluctuations across the pedaling normalized with respect to the total cycle for each condition and hemisphere. Curves are values averaged across the beta frequencies (13-35 Hz) of the time-frequency decompositions.
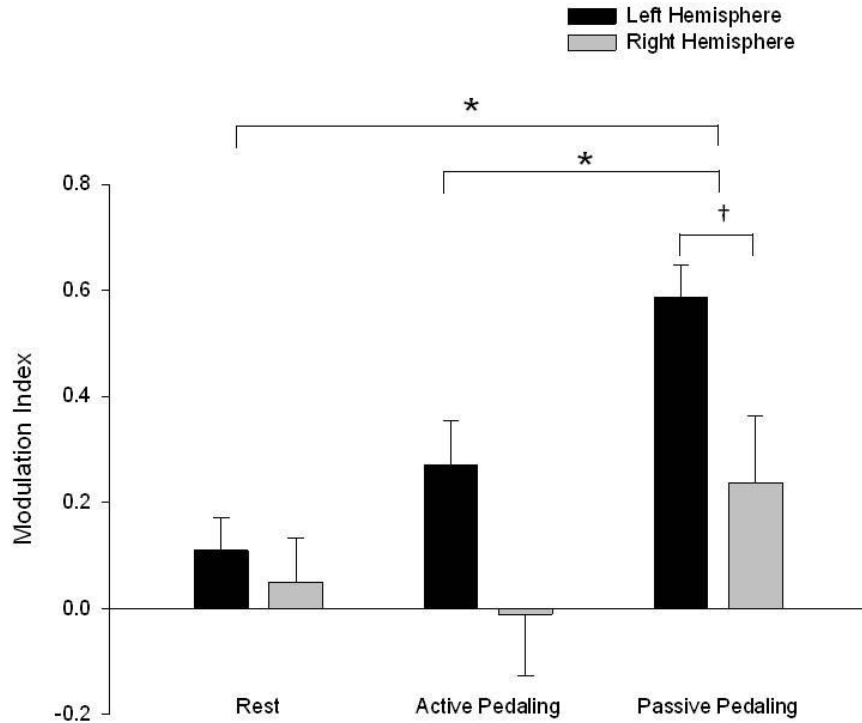
Figure 8. Symmetry indices calculated from the peak z-score values in the averaged envelopes. SI = flexion peak z-score – extension peak z-score. Si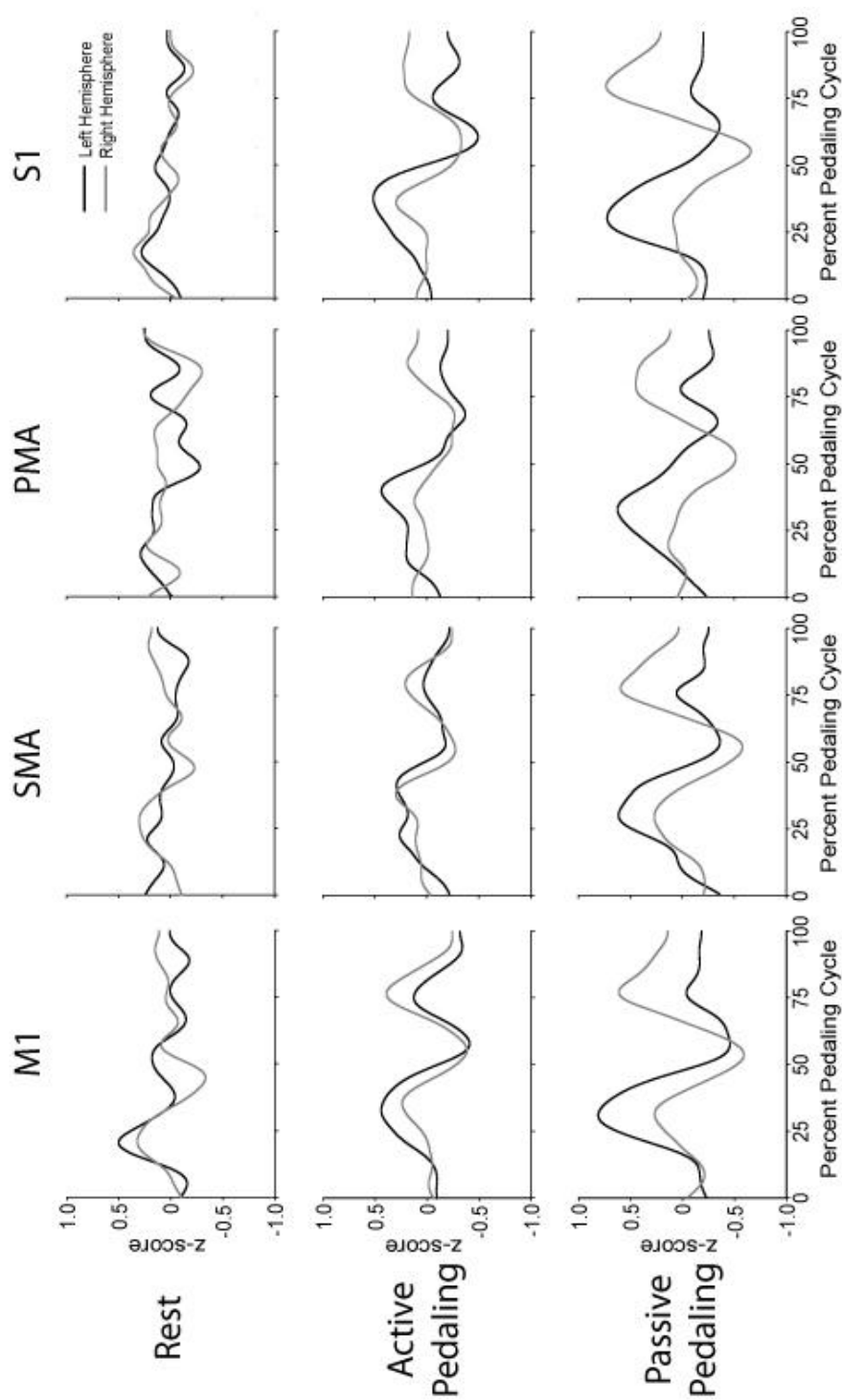gnificant differences between conditions expressed by *. Significant differences between hemispheres expressed by †. Error bars are standard error.

Table 2. Symmetry index values, mean (standard error), representing the amount a hemisphere modulates in the beta band between the flexion and extension phases for each condition.

	Rest	Active	Passive
Left Hemisphere	0.11(0.06)	0.27(0.08)	0.59(0.06)
Right Hemisphere	0.05(0.08)	-0.01(0.12)	0.24(0.13)

Despite no significant global effect of hemisphere (3-way ANOVA, parameters: condition, hemisphere, brain area), it was visually clear that the amount of modulation did vary with respect to hemisphere. Symmetry indices are found in Table 3. During passive pedaling, the symmetry indices for the left and right hemispheres were 0.586(0.061) and 0.237(0.127), respectively the mean (standard error). See Figure 8. These values were significantly different (P=0.016), suggesting that modulation of beta

power during passive pedaling was larger in the left as compared to the right hemisphere. A similar trend was apparent during active pedaling and rest. However, these observation did not reach statistical significance (P=0.054, P=0.132, respectively).

CHAPTER 4 – DISCUSSION

Our results show that the varying cortical magnetic signal can be recorded during a locomotor-like movement using MEG. Frequency analysis over the primary sensorimotor cortex, supplemental and premotor areas demonstrated a modulation pattern associated with the various phases of pedaling (flexion, extension, and transitions.)

4.1 DECREASE IN POWER DURING MOVEMENT

In all regions of interest, a significant decrease in power occurred in the alpha and beta bands during both active and passive pedaling as compared to rest. There was no significant difference between active and passive pedaling power. The gamma band did not show a significant drop in power from rest to movement.

The trends of alpha and beta power decrease compared to rest have been seen during isometric muscle contractions (Conway et al. 1995, Salenius et al. 1997), repetitive hand movements (Salmelin et al. 1995, Pfurtscheller et al. 1997, Gross et al. 2005, Erbil & Ungan 2007), and toe movements (Salmelin et al. 1995, Pfurtscheller et al. 1997). As mentioned previously, the decrease in power during movement corresponds to a desynchronization of neuronal populations. This could be a transition from idling neurons ready to be used into the functional firing of specific groups of neurons needed in a task.

While we did not see any difference in the gamma power between rest and movement, Huo et al. (2010) showed a gamma power contralateral increase and ipsilateral decrease in the motor areas with respect to index finger movement. Conway et

al. (1995) also showed an increase of the gamma band was maintained during low level isometric contractions of the first dorsal interosseous muscle. We most likely observed no difference in gamma power between movement and rest due to the size of the regions of interest we examined. The period of neural oscillations are constrained by the distance between the communicating groups of neurons. Thus, the lower frequency bands can occur in larger neuronal networks across the brain while the higher frequency bands, such as gamma, are more spatially focal (Buzsaki & Draguhn 2004, Huo et al. 2010).

4.2 BETA BAND MODULATION OF POWER ACROSS THE PEDALING CYCLE

The two pedaling conditions produced a clear modulation across the pedaling cycle as demonstrated in the normalized TFD envelopes of the beta band in Figure 5. The deep fluctuations occurred at approximately twice the pedaling rate in all regions of interest. The peaks of the fluctuations match up to the flex-/extension of the pedaling, while the locations of the valleys occur at the transition parts of the cycle. Since the y-axis is the z-score normalization of the signals' power, the positive and negative values correspond to power values that are higher or lower than the mean power. In other terms, it is the synchronization and desynchronization, respectively, of those cortical regions. The rest condition does not follow a distinct modulation pattern during a comparable period of time.

High temporal resolution recordings are necessary when examining cortical activity across various phases of a movement cycle. Movement noise artifacts have proven difficult to deal with in these high temporal resolution recordings. However, a few recent studies have been able to show sensorimotor modulation during continuous,

locomotor-like tasks using EEG. Electrocortical activity was recorded during treadmill

walking (Gwin et al. 2011), pedaling (Gourab et al., in review), and standardized gait-like

leg movements while in an upright position (Wieser et al. 2010). Indeed all three groups

showed that modulation of the movement related potentials (Wieser et al. 2010, Gourab

et al., in review) or event-related spectral perturbations, ERSP, (Gwin et al. 2011)

occurred over the motor areas, suggesting that the cortex does influence motor output.

Gourab (in review), Gwin (2011), and colleagues demonstrated modulation at twice the

movement frequency. Wieser (2010), Gourab (in review), and colleagues noted the

highest cortical involvement occurred at the transitions between flexion and extension

when a limb direction change occurred. On the other hand, Gwin et al. (2011) showed a

synchronization, or cortical deactivation, at the stance-to-swing transitions during

walking on a treadmill with EEG.

Modulation across the pedaling cycle demonstrates the cortex assists in the

control of locomotor output. While sensory input certainly has a large effect on cortical

activity, as can be noticed from the power spectra in Figure 3, there are definite

differences when comparing from just sensory to sensory and motor tasks. More on that

in the following section.

4.3 DIFFERENCES IN ACTIVE AND PASSIVE PEDALING BETA BAND
MODULATION

The power spectra show a similar amount of overall desynchronization in both

active and passive pedaling as compared to rest. However, adding the time component

with the TFDs demonstrated some variation between the pedaling conditions as relating

to the cycle phases. The value used to determine the variation in peak z-score value between upstroke and downstroke was the symmetry index (SI). The higher the SI, the more the z-score modulated across the pedaling cycle. When comparing pedaling conditions, the passive condition modulated significantly more than the active condition across the pedaling cycle. The passive certainly has a higher synchronization in one phase of the cycle as compared to the other, while the spectral power seems to become more symmetric when motor output is added with active pedaling. Despite these differences, both pedaling conditions express the highest desynchronization, or cortical activity, during the transition phases.

Cortical activity during locomotor-like movements has shown active and passive pedaling to be similar over the entire cycle in terms of PET activity (Christensen et al. 2000) and fMRI volume of activation (Mehta et al. 2012). There has not been much comparison between the two conditions throughout the different phases of locomotor-like cycles, once again due to artifacts and processing obstacles in high temporal recordings of EEG. Gourab et al. (in review) was able to look at phases of the pedaling cycle with EEG during active and passive pedaling. In the averaged EEG waveform over time, both pedaling conditions showed a similar modulation at twice the pedaling frequency. However, the passive task elicited a higher amplitude averaged waveform than active pedaling.

Our beta band data (Figure 5) is z-score normalized with respect to the entire cycle during that condition; thus the synchronizations and desynchronizations are compared to the average power in that condition. Thus it is harder to directly compare the power in the time-frequency plots between passive and active pedaling, but

generalizations can still be made about the increases and decreases in power of the beta band. During the passive pedaling cycle, the highest synchronization occurs while the contralateral leg is flexing during the upstroke. This suggests the higher cortical activation (desynchronization) is needed when the contralateral leg is passively being extended. This contradicts the idea that muscle spindle activity, and thus sensory input, increases when the muscle is stretched during flexion (Hulliger 1984).

On the other hand, the flexion and extension phases of the active pedaling cycle have a more similar amount of beta band power. The motor output could decrease the pure sensory effect and cause an evening out of the cortical activity during locomotor-like activity. It has been shown that somatosensory evoked potential decreases during walking as compared to standing (Duysens et al. 1995), referred to as sensory gating.

Regardless of a sensory and motor task or just sensory task, the highest cortical demands occur while the muscles are transitioning between flexion and extension.

4.4 HEMISPHERIC ASYMMETRY DURING PEDALING

The TFD averaged envelopes show a visible asymmetry between the left (LH) and right (RH) hemispheres in beta band power fluctuations. The left hemisphere has a higher symmetry index, which is most pronounced during passive pedaling in all regions and in S1 during active pedaling. It is also statistically significant for the passive condition.

While there is no solid evidence that one hemisphere dominates neural activity, theories exist that handedness corresponds to asymmetric neural control. It has been shown that the dominant hemisphere (contralateral to the dominant hand) has a larger

hand motor area activated during comparable movements of both hands (Volkmann 1998). Of course, it is hard to apply that explanation to our result since all of the subjects were right-handed and there was no left-handed data to compare.

CHAPTER 5 – CONCLUSION

The success of the first MEG pedaling experiment will help to lay the foundation in this area of study. We indeed saw task-related MEG signal during pedaling that was not seen during rest and was modulated with the phase of the pedaling cycle, suggesting that the sensory and motor cortices are involved in controlling locomotion. Also, the MEG signal had a similar power decrease during active and passive pedaling, but the modulation across time was different. This leads to the conclusion that locomotor-related brain activity is not solely caused by sensory feedback

5.1 FUTURE WORK

I have several recommendations for continuing work on this study.   It seems that the gamma band has importance in the control of locomotion and should be examined more in depth. As I did not apply the Morlet wavelet to frequencies higher than 50 Hz, I recommend looking at the low gamma band (35-80 Hz) and high gamma band (80-150 Hz). Examining the time-frequency component of the signal in these higher frequencies will give insight into the modulation of the gamma band across time.

Another change would be to look at the medial aspects of M1 and S1. The somatotopic control of the legs occurs in the medial portion of those areas and may lead to a clearer picture of locomotor-related activity.

An important measure to include in a future study would be EMG activity of the leg muscles. This will allow for corticomuscular coherence analysis, which is commonly examined in MEG movement studies. EMG data will also give a better gauge of the

amount of power the subject's are inputting during the passive movements.

 While this thesis lays the groundwork for pedaling studies in the MEG, these recommendations will take the experiments and conclusions much further.

BIBLIOGRAPHY

Alegre, M., de Gurtubay, I. G., Labarga, A., Iriarte, J., Malanda, A., & Artieda, J. (2004). Alpha and beta oscillatory activity during a sequence of two movements. *Clinical Neurophysiology*, 115(1), 124-130.

Baillet, S., Mosher, J. C., & Leahy, R. M. (2001). Electromagnetic brain mapping. *IEEE Signal Processing Magazine,* , 14-30.

Barbeau, H., & Rossignol, S. (1987). Recovery of locomotion after chronic spinalization in the adult cat. *Brain Research,* 412(1), 84-95.

Belanger, M., Drew, T., Provencher, J., & Rossignol, S. (1996). A comparison of treadmill locomotion in adult cats before and after spinal transection. *Journal of Neurophysiology*, 76(1), 471-491.

Bennett, M. V., & Zukin, R. S. (2004). Electrical coupling and neuronal synchronization in the mammalian brain. *Neuron*, 41(4), 495-511.

Berger, H. (1929). Über das Elektrenkephalogramm des Menschen. *European Archives of Psychiatry and Clinical Neuroscience*: 87(1), 527-570.

Boonstra, T. W., Daffertshofer, A., Breakspear, M., & Beek, P. J. (2007). Multivariate time-frequency analysis of electromagnetic brain activity during bimanual motor learning. *NeuroImage*, 36(2), 370-377.

Brown, D. A., & Kukulka, C. G. (1993). Human flexor reflex modulation during cycling. *Journal of Neurophysiology, 69*(4), 1212-1224.

Buzsaki, G., & Draguhn, A. (2004). Neuronal oscillations in cortical networks. *Science, 304*(5679), 1926-1929.

Calancie, B., Needham-Shropshire, B., Jacobs, P., Willer, K., Zych, G., & Green, B. A. (1994). Involuntary stepping after chronic spinal cord injury: Evidence for a central rhythm generator forlocomotion in man. *Brain : A Journal of Neurology, 117*(5), 1143-1159.

Capaday, C., Lavoie, B. A., Barbeau, H., Schneider, C., & Bonnard, M. (1999). Studies on the corticospinal control of human walking. I. responses to focal transcranial magnetic stimulation of the motor cortex. *Journal of Neurophysiology*, 81(1), 129-139.

Chen, R., Corwell, B., & Hallett, M. (1999). Modulation of motor cortex excitability by median nerve and digit stimulation. *Experimental Brain Research, 129*(1), 77-86.

Christensen, L. O., Johannsen, P., Sinkjaer, T., Petersen, N., Pyndt, H. S., & Nielsen, J. B. (2000). Cerebral activation during bicycle movements in man. *Experimental Brain Research,* 135(1), 66-72.

Ciccarelli, O., Toosy, A. T., Marsden, J. F., Wheeler-Kingshott, C. M., Sahyoun, C., Matthews, P. M., et al. (2005). Identifying brain regions for integrative sensorimotor processing with ankle movements. *Experimental Brain Research*, 166(1), 31-42.

Conway, B. A., Halliday, D. M., Farmer, S. F., Shahani, U., Maas, P., Weir, A. I., et al. (1995). Synchronization between motor cortex and spinal motoneuronal pool during the performance of a maintained motor task in man. *The Journal of Physiology*, 489 (Pt 3), 917-924.

Dietz, V., Colombo, G., Jensen, L., & Baumgartner, L. (1995). Locomotor capacity of spinal cord in paraplegic patients. *Annals of Neurology*, 37(5), 574-582.

Dietz, V., Faist, M., & Pierrot-Deseilligny, E. (1990). Amplitude modulation of the quadriceps H-reflex in the human during the early stance phase of gait. *Experimental Brain Research.,* 79(1), 221-224.

Dietz, V., & Harkema, S. J. (2004). Locomotor activity in spinal cord-injured persons. *Journal of Applied Physiology*, 96(5), 1954-1960.

Dimitrijevic, M. R., Gerasimenko, Y., & Pinter, M. M. (1998). Evidence for a spinal central pattern generator in humans. *Annals of the New York Academy of Sciences:860*, 360-376.

Drew, T. (1988). Motor cortical cell discharge during voluntary gait modification. *Brain Research*, 457(1), 181-187.

Drew, T. (1993). Motor cortical activity during voluntary gait modifications in the cat. I. cells related to the forelimbs. *Journal of Neurophysiology*, 70(1), 179-199.

Drew, T., Jiang, W., Kably, B., & Lavoie, S. (1996). Role of the motor cortex in the control of visually triggered gait modifications. *Canadian Journal of Physiology and Pharmacology*, 74(4), 426-442.

Drew, T., Jiang, W., & Widajewicz, W. (2002). Contributions of the motor cortex to the control of the hindlimbs during locomotion in the cat. *Brain Research. Brain Research Reviews,* 40(1-3), 178-191.

Duysens, J., & Pearson, K. G. (1980). Inhibition of flexor burst generation by loading ankle extensor muscles in walking cats. *Brain Research, 187*(2), 321-332.

Duysens, J., Tax, A. A., Nawijn, S., Berger, W., Prokop, T., & Altenmuller, E. (1995).

Gating of sensation and evoked potentials following foot stimulation during human gait. *Experimental Brain Research, 105*(3), 423-431.

Duysens, J., & Van de Crommert, H. W. (1998). Neural control of locomotion; the central pattern generator from cats to humans. *Gait & Posture*, 7(2), 131-141.

Erbil, N., & Ungan, P. (2007). Changes in the alpha and beta amplitudes of the central EEG during the onset, continuation, and offset of long-duration repetitive hand movements. *Brain Research*, 1169, 44-56.

Faist, M., Dietz, V., & Pierrot-Deseilligny, E. (1996). Modulation, probably presynaptic in origin, of monosynaptic Ia excitation during human gait. *Experimental Brain Research*, 109(3), 441-449.

Ferris, D. P., Gordon, K. E., Beres-Jones, J. A., & Harkema, S. J. (2004). Muscle activation during unilateral stepping occurs in the nonstepping limb of humans with clinically complete spinal cord injury. *Spinal Cord, 42*(1), 14-23.

Fukuyama, H., Ouchi, Y., Matsuzaki, S., Nagahama, Y., Yamauchi, H., Ogawa, M., et al. (1997). Brain functional activity during gait in normal subjects: A SPECT study. *Neuroscience Letters,228*(3), 183-186.

Gourab, K., Jain, S., Schindler-Ivens, S., Schmit, B.D. EEG during pedaling: evidence for cortical control of locomotor tasks. In Review.

Grillner, S., & Rossignol, S. (1978). On the initiation of the swing phase of locomotion in chronic spinal cats. *Brain Research*, 146(2), 269-277.

Grillner, S., & Zangger, P. (1975). How detailed is the central pattern generation for locomotion? *Brain Research*, 88(2), 367-371.

Gross, J., Pollok, B., Dirks, M., Timmermann, L., Butz, M., & Schnitzler, A. (2005). Task-dependent oscillations during unimanual and bimanual movements in the human primary motor cortex and SMA studied with magnetoencephalography. *NeuroImage*, 26(1), 91-98.

Guertin, P., Angel, M. J., Perreault, M. C., & McCrea, D. A. (1995). Ankle extensor group I afferents excite extensors throughout the hindlimb during fictive locomotion in the cat. *The Journal of Physiology,* 487 (Pt 1)(Pt 1), 197-209.

Gwin, J. T., Gramann, K., Makeig, S., & Ferris, D. P. (2011). Electrocortical activity is coupled to gait cycle phase during treadmill walking. *NeuroImage*, 54(2), 1289-1296.

Hamalainen, M., Hari, R., Ilmoniemi, R.J., Knuutila, J., & Lounasmaa, O.V. (1993). Magnetoencephalography – theory, instrumentation, and applications to noninvasive

studies of the working human brain. *Reviews of Modern Physics*, 65(2), 413-497.

Hari, R. & Salmelin, R. (2012). Magnetoencephalography: From SQUIDs to neuroscience. *NeuroImage*, 61(2), 386-96.

Hiebert, G. W., Whelan, P. J., Prochazka, A., & Pearson, K. G. (1996). Contribution of hind limb flexor muscle afferents to the timing of phase transitions in the cat step cycle. *Journal of Neurophysiology, 75*(3), 1126-1137.

Holmes, C. J., Hoge, R., Collins, L., Woods, R., Toga, A. W., & Evans, A. C. (1998). Enhancement of MR images using registration for signal averaging. *Journal of Computer Assisted Tomography*, 22(2), 324-333.

Huang, M. X., Mosher, J. C., & Leahy, R. M. (1999). A sensor-weighted overlapping sphere head model and exhaustive head model comparison for MEG. *Physics in Medicine and Biology, 44*(2), 423-440.

Hulliger, M. (1984). The mammalian muscle spindle and its central control. *Reviews of Physiology, Biochemistry and Pharmacology, 101*, 1-110.

Huo, X., Xiang, J., Wang, Y., Kirtman, E. G., Kotecha, R., Fujiwara, H., et al. (2010). Gamma oscillations in the primary motor cortex studied with MEG. *Brain & Development, 32*(8), 619-624.

Hutchison, W. D., Dostrovsky, J. O., Walters, J. R., Courtemanche, R., Boraud, T., Goldberg, J., et al. (2004). Neuronal oscillations in the basal ganglia and movement disorders: Evidence from whole animal and human recordings. *The Journal of Neuroscience:* 24(42), 9240-9243.

Iles, J. F. (1996). Evidence for cutaneous and corticospinal modulation of presynaptic inhibition of ia afferents from the human lower limb. *The Journal of Physiology, 491* (Pt 1), 197-207.

Lam, T., & Pearson, K. G. (2001). Proprioceptive modulation of hip flexor activity during the swing phase of locomotion in decerebrate cats. *Journal of Neurophysiology*, 86(3), 1321-1332.

Marder, E., & Calabrese, R. L. (1996). Principles of rhythmic motor pattern generation. *Physiological Reviews*, 76(3), 687-717.

Mehta, J. P., Verber, M. D., Wieser, J. A., Schmit, B. D., & Schindler-Ivens, S. M. (2012). The effect of movement rate and complexity on functional magnetic resonance signal change during pedaling. *Motor Control*, 16(2), 158-175.

Miyai, I., Tanabe, H. C., Sase, I., Eda, H., Oda, I., Konishi, I., et al. (2001). Cortical mapping of gait in humans: A near-infrared spectroscopic topography study.

NeuroImage, 14(5), 1186-1192.

Nielsen, J. B. (2003). How we walk: Central control of muscle activity during human walking. *The Neuroscientist 9*(3), 195-204.

Pearson, K. G. (1995). Proprioceptive regulation of locomotion. *Current Opinion in Neurobiology, 5*(6), 786-791.

Petersen, N., Christensen, L. O., & Nielsen, J. (1998). The effect of transcranial magnetic stimulation on the soleus H reflex during human walking. *The Journal of Physiology, 513* (Pt 2), 599-610.

Petersen, N. T., Butler, J. E., Marchand-Pauvert, V., Fisher, R., Ledebt, A., Pyndt, H. S., et al. (2001). Suppression of EMG activity by transcranial magnetic stimulation in human subjects during walking. *The Journal of Physiology, 537*(Pt 2), 651-656.

Pfurtscheller, G., Neuper, C., Andrew, C., & Edlinger, G. (1997). Foot and hand area mu rhythms. *International Journal of Psychophysiology* 26(1-3), 121-135.

Raethjen, J., Govindan, R. B., Binder, S., Zeuner, K. E., Deuschl, G., & Stolze, H. (2008). Cortical representation of rhythmic foot movements. *Brain Research*, 1236, 79-84.

Rossignol, S. (2000). Locomotion and its recovery after spinal injury. *Current Opinion in Neurobiology, 10*(6), 708-716.

Rossignol, S., Drew, T., Brustein, E., & Jiang, W. (1999). Locomotor performance and adaptation after partial or complete spinal cord lesions in the cat. *Progress in Brain Research, 123*, 349-365.

Rossignol, S., & Frigon, A. (2011). Recovery of locomotion after spinal cord injury: Some facts and mechanisms. *Annual Review of Neuroscience, 34*, 413-440.

Sahyoun, C., Floyer-Lea, A., Johansen-Berg, H., & Matthews, P. M. (2004). Towards an understanding of gait control: Brain activation during the anticipation, preparation and execution of foot movements. *NeuroImage, 21*(2), 568-575.

Salenius, S., Portin, K., Kajola, M., Salmelin, R., & Hari, R. (1997). Cortical control of human motoneuron firing during isometric contraction. *Journal of Neurophysiology, 77*(6), 3401-3405.

Salmelin, R., Hamalainen, M., Kajola, M., & Hari, R. (1995). Functional segregation of movement-related rhythmic activity in the human brain. *NeuroImage, 2*(4), 237-243.

Sahyoun, C., Floyer-Lea, A., Johansen-Berg, H., & Matthews, P. M. (2004). Towards an understanding of gait control: Brain activation during the anticipation, preparation

and execution of foot movements. *NeuroImage, 21*(2), 568-575.

Schnitzler, A., & Gross, J. (2005). Normal and pathological oscillatory communication in the brain. *Nature Reviews.Neuroscience, 6*(4), 285-296.

Schubert, M., Curt, A., Jensen, L., & Dietz, V. (1997). Corticospinal input in human gait: Modulation of magnetically evoked motor responses. *Experimental Brain Research. 115*(2), 234-246.

Shik, M. L., Severin, F. V., & Orlovsky, G. N. (1966). Control of walking and running by means of electrical stimulation of the mid-brain. *Biophysics, 11*, 756-765.

Sidhu, S. K., Hoffman, B. W., Cresswell, A. G., & Carroll, T. J. (2012). Corticospinal contributions to lower limb muscle activity during cycling in humans. *Journal of Neurophysiology, 107*(1), 306-314.

Stephens, M. J., & Yang, J. F. (1996a). The effects of load on the human step cycle. *Society for Neuroscience Abstracts, 22*, 726-728.

Stephens, M. J., & Yang, J. F. (1996b). Short latency, non-reciprocal group I inhibition is reduced during the stance phase of walking in humans. *Brain Research, 743*(1), 24-31.

Stephens, M. J., & Yang, J. F. (1999). Loading during the stance phase of walking in humans increases the extensor EMG amplitude but does not change the duration of the step cycle. *Experimental Brain 124*(3), 363-370.

Steriade, M., & Llinas, R. R. (1988). The functional states of the thalamus and the associated neuronal interplay. *Physiological Reviews, 68*(3), 649-742.

Steriade, M., McCormick, D. A., & Sejnowski, T. J. (1993). Thalamocortical oscillations in the sleeping and aroused brain. *Science, 262*(5134), 679-685.

Tadel, F., Baillet, S., Mosher, J. C., Pantazis, D., & Leahy, R. M. (2011). Brainstorm: A user-friendly application for MEG/EEG analysis. *Computational Intelligence and Neuroscience,* 2011, 879-716.

Tallon-Baudry, C. & Bertrand, O. (1999). Oscillatory gamma activity in humans and its role in object representation. *Trends in Cognitive Sciences*, 3(4), 151-162.

Taulu S., Simola, J., & Kajola, M. (2004). MEG recordings of DC fields using the signal space separation method (SSS). *Neurology and Clinical Neurophysiology*, 35.

Volkmann, J. (1998). Oscillations of the human sensorimotor system as revealed by magnetoencephalography. *Movement Disorders : 13 Suppl 3*, 73-76.

Whelan, P. J., Hiebert, G. W., & Pearson, K. G. (1995). Stimulation of the group I extensor afferents prolongs the stance phase in walking cats. *Experimental Brain Research*. 103(1), 20-30.

Wieser, M., Haefeli, J., Butler, L., Jancke, L., Riener, R., & Koeneke, S. (2010). Temporal and spatial patterns of cortical activation during assisted lower limb movement. *Experimental Brain Research. 203*(1), 181-191.

Wu, M., Gordon, K., Kahn, J. H., & Schmit, B. D. (2011). Prolonged electrical stimulation over hip flexors increases locomotor output in human SCI. *Clinical Neurophysiology :122*(7), 1421-1428.

Yang, J. F., Stephens, M. J., & Vishram, R. (1998). Transient disturbances to one limb produce coordinated, bilateral responses during infant stepping. *Journal of Neurophysiology, 79*(5), 2329-2337.

Zehr, E. P., & Stein, R. B. (1999). What functions do reflexes serve during human locomotion? *Progress in Neurobiology, 58*(2), 185-205.

APPENDIX A - MATLAB codes

Appendix A.1 Extracting the event files from the optical encoder position data.

'bst_extract_fif_channel.'

This script is adapted from the Brainstorm program and customized to the pedaling protocol. Necessary inputs are *rawFile* and *ChannelName.* See descriptions below.

```
function Data = bst_extract_fif_channel(rawFile,ChannelName)
%  bst_extract_fif_channel: reads out data time series from selected
%  channels from a raw fiff file
%
% Usage:
%
%     Data = bst_extract_fif_channel(rawFile,ChannelName);
%
% Description:
%
%     rawFile: file name of the raw fif file to be read
%     ChannelName: a cell array of N channel name(s) to be read from
file
%
%     Data: an array with N rows, each row in the order of the channels
specified in ChannelName
%


%% -- Define fiff read parameters
allow_maxshield = 1;


%% -- Extract selected channel time series from raw fiff file
rawStruct = fiff_setup_read_raw(rawFile, allow_maxshield);
time_in =  double(rawStruct.first_samp) / double(rawStruct.info.sfreq);
% recording begins
time_out = double(rawStruct.last_samp) / double(rawStruct.info.sfreq);
% recording ends
[sel] = fiff_pick_channels(rawStruct.info.ch_names,ChannelName,[]);
[Data,times] =
fiff_read_raw_segment_times(rawStruct,time_in,time_out,sel);

%% -- Compute time derivatives of extracted time series
dDatadt = diff(Data(1,:));
%xf = bandpassFilter(Data(2,:),rawStruct.info.sfreq,30,40);

%% -- Define events at extrema of the time derivative series
%[mdDatadt, indMax] = max(abs(dDatadt));
[XMAX,IMAX,XMIN,IMIN] = extrema(abs(dDatadt));
[N,X]=hist(XMAX, 2);
iEvent = find(abs(dDatadt)>X(end)); % Detect maxima - may need some
extra cleaning
iEvent(diff(iEvent)<10)=[];
iEvent(iEvent<=rawStruct.first_samp) = [];

%iEvent = find(Data(2,:)>.995*XMAX(1)); % Detect maxima - may need some
extra cleaning
```

```
%% - Create an event file corresponding to maxima
%eventArray = zeros(2*length(iEvent),4);
eventArray(1,:) = [double(rawStruct.first_samp),
double(rawStruct.first_samp) / double(rawStruct.info.sfreq), 0, 0]; %
Start of recording
idEvent = ceil(diff(iEvent)/2); % half-cycle latencies
for k = 1:length(iEvent)
    eventArray(end+1,:) = double([iEvent(k), double(iEvent(k)) /
double(rawStruct.info.sfreq), 0 , 1]);
    if k<length(iEvent)
        eventArray(end+1,:) = double([iEvent(k)+idEvent(k),
double((iEvent(k)+idEvent(k))) / double(rawStruct.info.sfreq), 0 , 2]);
    end
end



figure, plot(Data'), hold on,
plot(eventArray(eventArray(:,4)==1),Data(1,eventArray(eventArray(:,4)==
1)),'ro'),
plot(eventArray(eventArray(:,4)==2),Data(1,eventArray(eventArray(:,4)==
2)),'b+'),

eventArray(:,1) = eventArray(:,1)+double(rawStruct.first_samp);
eventArray(:,2) = eventArray(:,2)+double(time_in);

eventFile = strrep(rawFile,'.fif','_auto.eve');
feve = fopen(eventFile,'wt');
fprintf(feve,'%d %6.3f %d %d\n',eventArray');
fclose(feve);
```

Appendix A.2 Splitting data into pedaling cycles, spline interpolation, and loading into Brainstorm.

```matlab
%Load the Event text file and select only the Event 1 starting times
Events = load('*.eve file path');
Event_Ones = find(Events(:,4)==1);
StartTimes = Events(Event_Ones,1);

%calculate the length of each cycle
CycleLength = diff(StartTimes);

fiffheader=fiff_setup_read_raw('*.fif file path');

%loop from StartTimes(i) to StarTimes(i+1)
for i = 1:40
     data{i} =
fiff_read_raw_segment(fiffheader,StartTimes(i),StartTimes(i+1));
     NewFs(i) = (1000*2000)./(size(data{i},2));
end

for j = 1:size(data,2)
    x = 0:1/(size(data{j},2)-1):1;
    x = x*100;
    y = data{j};
    x1 = 0:.1:100-.1;
    %spline is fit to the signal and resampled at give number of
equally
    %spaced time points (or in this case percent of gait cycle)
    new_signal = interp1(x,y',x1,'spline');
    cycles_11(:,:,j) = new_signal';
end

%concatenates 2 cycles in order to make 1 epoch
for k=1:size(cycles_11,3)-1
    A=cycles_11(:,:,k);
    B=cycles_11(:,:,k+1);
    d(:,:,k)=cat(2, A,B);
    Fs(k) = (NewFs(k)+NewFs(k+1))/2;
    step(k) = 1/Fs(k);
end

% sends the newly formed epochs to BST
for i = 1:size(d,3)
     x.F = d(:,:,i);%imports channel x time matrices for each cycle
    x.Comment = ['Resting Epoch ' int2str(i+size(d,3)*4)];  %label in
BST
    x.Time = 0:step(i):2000/Fs(i)-1/Fs(i);
    x.ChannelFlag = ones(nchannels,1);
    x.Device = 'Neuromag';
    x.nAvg = 1; % only 1 epoch per structure
    x.DataType = 'recordings';
    filename = ['temporary file name '.mat'];
    save(filename, '-struct', 'x');
    import_data(filename, 'BST-MAT',69,9); %Study #, Subject #
end
```

Appendix A.3 - Calculations of the power spectra using the Welch periodogram.

'*spec.m*'
Script must be run for each subject and each brain area. Spectra can then be averaged across subjects.

```
rest_LH = resting_L.Value;
rest_RH = resting_R.Value;

pass_LH = passive_L.Value;
pass_RH = passive_R.Value;

act_LH = active_L.Value;
act_RH = active_R.Value;

Fs = 2000;

%resting spectra
[Axx, f] = pwelch(rest_LH,2000,1000,length(rest_LH),Fs,'onesided');
[Bxx, f] = pwelch(rest_RH,2000,1000,length(rest_RH),Fs,'onesided');

%passive spectra
[Cxx, f] = pwelch(pass_LH,2000,1000,length(pass_LH),Fs,'onesided');
[Dxx, f] = pwelch(pass_RH,2000,1000,length(pass_RH),Fs,'onesided');

%active spectra
[Exx, f] = pwelch(act_LH,2000,1000,length(act_LH),Fs,'onesided');
[Fxx, f] = pwelch(act_RH,2000,1000,length(act_RH),Fs,'onesided');

% LH_M1 resting vs. passive
N = figure;
subplot(2,1,1), plot(f,Axx,'r')
hold on, plot(f,Cxx,'k')
title('Left M1'),legend('Rest','Passive')
xlabel('Frequency (Hz)')
ylabel('|Y(f)|')
xlim([0 50])
ylim([0 2e-23])


% RH_M1 resting vs. passive
subplot(2,1,2),plot(f,Bxx,'r')
hold on, plot(f,Dxx,'k')
title('Right M1'),legend('Rest','Passive')
xlabel('Frequency (Hz)')
ylabel('|Y(f)|')
xlim([0 50])
ylim([0 2e-23])
```

Appendix A.4 - Calculations of average envelopes of time-frequency decompositions from Brainstorm.

'smooth.m'

Script passes envelope curves through a low-pass butterworth filter.

```
LH_rest = load ('C:/Documents and
Settings/1945swedler/Desktop/TFDenvelopes/
SMA/resting/LH_SMA_resting_C10.mat'); LH_rest = LH_rest.l_beta_C10;
RH_rest = load ('C:/Documents and
Settings/1945swedler/Desktop/TFDenvelopes/
SMA/resting/RH_SMA_resting_C10.mat'); RH_rest = RH_rest.r_beta_C10;
LH_act = load ('C:/Documents and
Settings/1945swedler/Desktop/TFDenvelopes/
SMA/active/LH_SMA_active_C10.mat'); LH_act = LH_act.l_beta_C10;
RH_act = load ('C:/Documents and
Settings/1945swedler/Desktop/TFDenvelopes/
SMA/active/RH_SMA_active_C10.mat'); RH_act = RH_act.r_beta_C10;
LH_pass = load ('C:/Documents and
Settings/1945swedler/Desktop/TFDenvelopes/
SMA/passive/LH_SMA_passive_C10.mat'); LH_pass = LH_pass.l_beta_C10;
RH_pass = load ('C:/Documents and
Settings/1945swedler/Desktop/TFDenvelopes/
SMA/passive/RH_SMA_passive_C10.mat'); RH_pass = RH_pass.r_beta_C10;


f = 1000; % sampling frequency for each subject
fc = 5; %cutoff frequency - Hz
fnorm = fc/(f/2);
[b1,a1] = butter(2,fnorm,'low'); %5th order Butterworth filter
lp_LH_rest = filtfilt(b1,a1,LH_rest); save 'C:/Documents and Settings/
1945swedler/Desktop/TFDenvelopes/SMA/new/resting/low_passed_LH_SMA_rest
ing_C10.mat' lp_LH_rest;
lp_LH_act = filtfilt(b1,a1,LH_act); save 'C:/Documents and Settings/
1945swedler/Desktop/TFDenvelopes/SMA/new/active/low_passed_LH_SMA_activ
e_C10.mat' lp_LH_act;
lp_LH_pass = filtfilt(b1,a1,LH_pass); save 'C:/Documents and Settings/
1945swedler/Desktop/TFDenvelopes/SMA/new/passive/low_passed_LH_SMA_pass
ive_C10.mat' lp_LH_pass;



lp_RH_rest = filtfilt(b1,a1,RH_rest); save 'C:/Documents and
Settings/1945swedler/Desktop/TFDenvelopes/SMA/new/resting/low_passed_RH
_SMA_resting_C10.mat' lp_RH_rest;
lp_RH_act = filtfilt(b1,a1,RH_act);save 'C:/Documents and
Settings/1945swedler/Desktop/TFDenvelopes/SMA/new/active/low_passed_RH_
SMA_active_C10.mat' lp_RH_act;
lp_RH_pass = filtfilt(b1,a1,RH_pass);save 'C:/Documents and
Settings/1945swedler/Desktop/TFDenvelopes/SMA/new/passive/low_passed_RH
_SMA_passive_C10.mat' lp_RH_pass;
```

```
x=0:.1:100-.1;
M = figure;
subplot(3,1,1), plot(x,LH_rest,'b:'),title('C10 SMA - resting')
hold on,
plot(x,lp_LH_rest,'b'),plot(x,RH_rest,'r:'),plot(x,lp_RH_rest,'r')
legend('LH','low passed LH','RH','low passed RH');


subplot(3,1,2), plot(x,LH_act,'b:'),title('active')
hold on,
plot(x,lp_LH_act,'b'),plot(x,RH_act,'r:'),plot(x,lp_RH_act,'r')

subplot(3,1,3), plot(x,LH_pass,'b:'),title('passive')
hold on,
plot(x,lp_LH_pass,'b'),plot(x,RH_pass,'r:'),plot(x,lp_RH_pass,'r')

saveas(M, ['C:/Documents and
Settings/1945swedler/Desktop/TFDenvelopes/SMA/new/low_passed_SMA_envelo
pes_C10.jpg']);
```

APPENDIX B – SPSS Statistical Outputs

APPENDIX B.1 – SPSS Output for Power Spectra Data (Result Section 3.1)

Univariate 3-way ANOVA
Dependent Variable: Mean Power
Fixed Factors: Condition, Frequency
Random Factors: Subject, Brain Area

Between-Subjects Factors

		N
frequency	alpha	192
	beta	192
	gamma	192
condition	active	192
	passive	192
	rest	192
Subject	C01	72
	C02	72
	C03	72
	C06	72
	C07	72
	C08	72
	C09	72
	C10	72
Brain Area	LH_M1	72
	LH_PMA	72
	LH_S1	72
	LH_SMA	72
	RH_M1	72
	RH_PMA	72
	RH_S1	72
	RH_SMA	72

Source		Type III Sum of Squares	df	Mean Square	F	Sig.
Intercept	Hypothesis	52766.779	1	52766.779	11.374	.008
	Error	44402.946	9.571	4639.265[a]		
frequency	Hypothesis	49074.032	2	24537.016	7.116	.006
	Error	57940.053	16.803	3448.154[b]		
condition	Hypothesis	9659.410	2	4829.705	3.479	.057
	Error	20986.541	15.116	1388.351[c]		
Subject	Hypothesis	26397.388	7	3771.055	1.092	.418
	Error	48742.440	14.113	3453.762[d]		
BrainArea	Hypothesis	8578.798	7	1225.543	1.625	.198
	Error	12194.320	16.168	754.234[e]		

frequency * condition	Hypothesis	12277.382	4	3069.345	2.870	.040
	Error	31312.016	29.273	1069.637^f		
frequency * Subject	Hypothesis	43233.275	14	3088.091	2.738	.009
	Error	37276.874	33.053	1127.783^g		
frequency * BrainArea	Hypothesis	8418.891	14	601.349	2.130	.030
	Error	11881.075	42.077	282.368^h		
condition * Subject	Hypothesis	18346.039	14	1310.431	1.235	.303
	Error	31252.885	29.461	1060.807^i		
condition * BrainArea	Hypothesis	3531.226	14	252.230	1.171	.346
	Error	6203.347	28.800	215.393^j		
Subject * BrainArea	Hypothesis	17509.312	49	357.333	1.306	.147
	Error	20323.001	74.297	273.538^k		
frequency * condition * Subject	Hypothesis	28799.561	28	1028.556	7.240	.000
	Error	27843.712	196	142.060^l		
frequency * condition * BrainArea	Hypothesis	5127.954	28	183.141	1.289	.162
	Error	27843.712	196	142.060^l		
frequency * Subject * BrainArea	Hypothesis	23646.086	98	241.287	1.698	.001
	Error	27843.712	196	142.060^l		
condition * Subject * BrainArea	Hypothesis	17082.491	98	.	.	.
	Error	.	.	.^{m}		
frequency * condition * Subject * BrainArea	Hypothesis	27843.712	196	142.060	.	.
	Error	.000	0	.^{n}		

Estimated Marginal Means of Mean Power
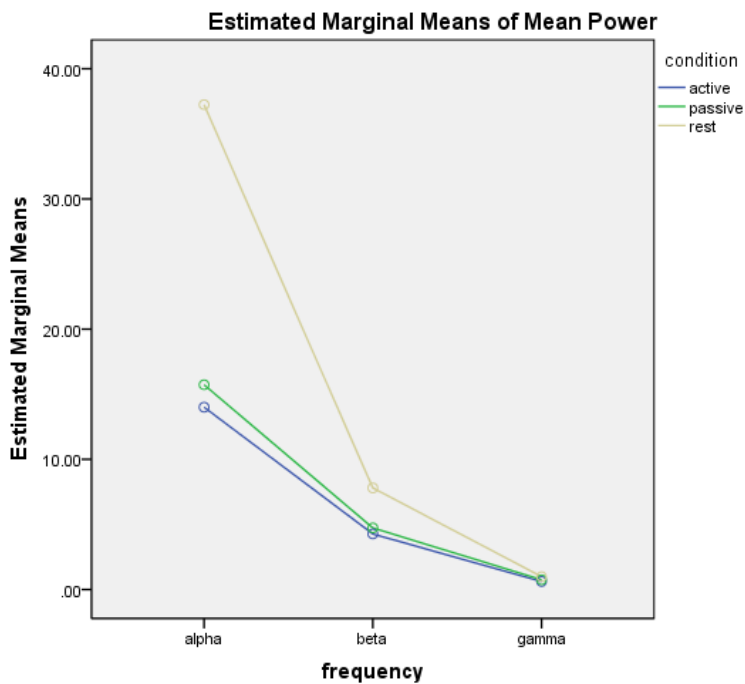
SUMMARY:
From the 3-way ANOVA, we see that there is a significant interaction between frequency and condition (p=.040). Also, there is no significant effect of Subjects or Brain Areas (p=.418, p=.198), so we are able to combine all those variables to get the resulting figure (to the left), which is Figure 3 in the thesis text.

Check to Combine Hemispheres

There needed to be no Hemisphere * Brain Area to validate the combining of Left and Right Hemispheres. There indeed was no interaction (p=.166)

Tests of Between-Subjects Effects

Dependent Variable:Mean Power

Source		Type III Sum of Squares	df	Mean Square	F	Sig.
Intercept	Hypothesis	52766.779	1	52766.779	19.498	.019
	Error	8625.750	3.187	2706.278[a]		
frequency	Hypothesis	49074.032	2	24537.016	17.801	.002
	Error	9212.497	6.683	1378.413[b]		
condition	Hypothesis	9659.410	2	4829.705	8.369	.018
	Error	3540.663	6.135	577.102[c]		
Area	Hypothesis	360.440	1	360.440	1.130	.368
	Error	923.593	2.895	318.990[d]		
BA	Hypothesis	7627.937	3	2542.646	1.665	.263
	Error	10339.903	6.770	1527.276[e]		
Area * BA	Hypothesis	590.421	3	196.807	2.377	.166
	Error	510.479	6.166	82.783[k]		

Alpha Band Simple Effects (1-way ANOVA) & Post Hocs

Descriptive Statistics

Dependent Variable:Mean Power

| condition	Mean	Std. Deviation	N
active	14.0036	15.91485	64
passive	15.7290	16.67144	64
rest	37.2436	55.02080	64
Total	22.3254	35.86232	192

Tests of Between-Subjects Effects

Dependent Variable:Mean Power

Source	Type III Sum of Squares	df	Mean Square	F	Sig.
Corrected Model	21460.280[a]	2	10730.140	9.046	.000
Intercept	95697.264	1	95697.264	80.678	.000
condition	21460.280	2	10730.140	9.046	.000
Error	224186.024	189	1186.169		
Total	341343.568	192			
Corrected Total	245646.304	191			

Multiple Comparisons

Dependent Variable:Mean Power

	(I) condition	(J) condition	Mean Difference (I-J)	Std. Error	Sig.	95% Confidence Interval	
						Lower Bound	Upper Bound
Tukey HSD	active	passive	-1.7255	6.08833	.957	-16.1081	12.6571
		rest	-23.2400*	6.08833	.001	-37.6226	-8.8574
	passive	active	1.7255	6.08833	.957	-12.6571	16.1081
		rest	-21.5145*	6.08833	.001	-35.8972	-7.1319
	rest	active	23.2400*	6.08833	.001	8.8574	37.6226
		passive	21.5145*	6.08833	.001	7.1319	35.8972

Estimated Marginal Means of Mean Power
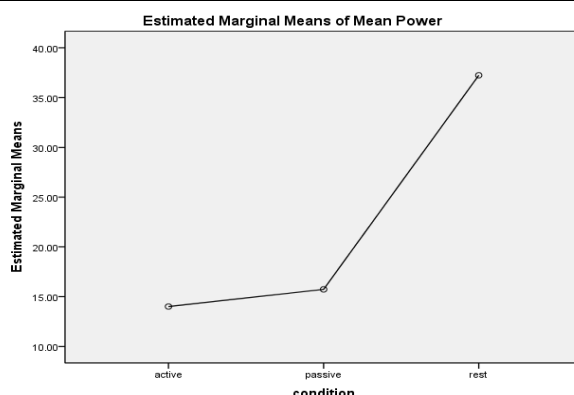
SUMMARY:
The Alpha band had a significant condition effect (p<.001), thus the Tukey post hocs were computed comparing each condition:

   Active *Rest - p = .001
   Passive * Rest - p=.001
   Active * Passive - p=.957

Both pedaling conditions (passive and active) are significantly different than rest in the alpha band. Passive and Active are not significant between each other.

Beta Band Simple Effects (1-way ANOVA) & Post Hocs

Descriptive Statistics

Dependent Variable:Mean Power

| condition	Mean	Std. Deviation	N
active	4.2689	4.12395	64
passive	4.7333	4.48534	64
rest	7.8028	5.41652	64
Total	5.6017	4.93902	192

Tests of Between-Subjects Effects

Dependent Variable:Mean Power

Source	Type III Sum of Squares	df	Mean Square	F	Sig.
Corrected Model	472.008^a	2	236.004	10.653	.000
Intercept	6024.716	1	6024.716	271.939	.000
condition	472.008	2	236.004	10.653	.000
Error	4187.230	189	22.155		
Total	10683.954	192			
Corrected Total	4659.238	191			

Multiple Comparisons

Dependent Variable:Mean Power

	(I) condition	(J) condition	Mean Difference (I-J)	Std. Error	Sig.	95% Confidence Interval	
						Lower Bound	Upper Bound
Tukey HSD	active	passive	-.4644	.83207	.842	-2.4300	1.5013
		rest	-3.5338*	.83207	.000	-5.4994	-1.5682
	passive	active	.4644	.83207	.842	-1.5013	2.4300
		rest	-3.0695*	.83207	.001	-5.0351	-1.1039
	rest	active	3.5338*	.83207	.000	1.5682	5.4994
		passive	3.0695*	.83207	.001	1.1039	5.0351

Estimated Marginal Means of Mean Power
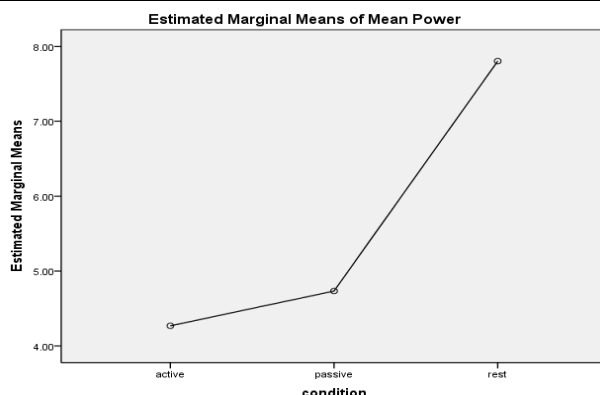
SUMMARY:
The Beta band had a significant condition effect (p<.001), thus the Tukey post hocs were computed comparing each condition:

Active *Rest - p < .001
Passive * Rest - p=.001
Active * Passive - p=.842

Both pedaling conditions (passive and active) are significantly different than rest in the beta band. Passive and Active are not significant between each other.

Gamma Band Simple Effects (1-way ANOVA)

Descriptive Statistics

Dependent Variable:Mean Power

condition	Mean	Std. Deviation	N
active	.6197	.60905	64
passive	.7507	1.03312	64
rest	.9897	.89856	64
Total	.7867	.87425	192

Tests of Between-Subjects Effects

Dependent Variable:Mean Power

Source	Type III Sum of Squares	df	Mean Square	F	Sig.
Corrected Model	4.504[a]	2	2.252	3.009	.052
Intercept	118.831	1	118.831	158.745	.000
condition	4.504	2	2.252	3.009	.052
Error	141.478	189	.749		
Total	264.814	192			
Corrected Total	145.983	191			

SUMMARY:

The Gamma band did not have a significant condition effect (p=.052), thus no post hocs were performed.

PMA 2-way ANOVA

The Premotor Area freq*cond plots looked as if there might not be a significant interaction. A 2-way ANOVA was performed to determine significance.
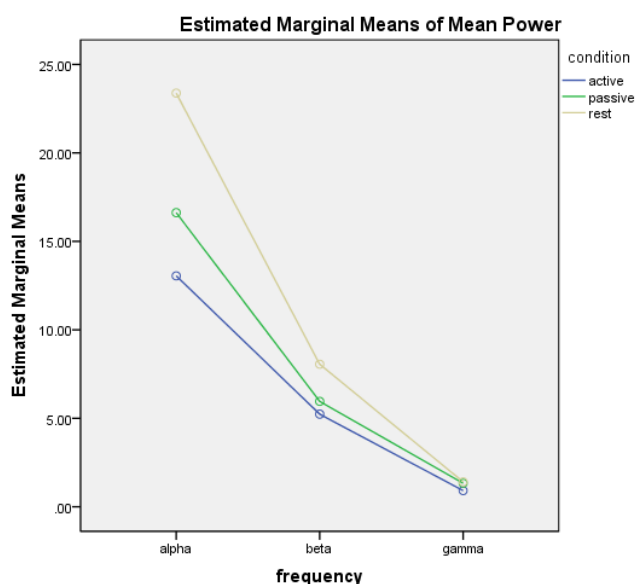
Between-Subjects Factors

		N
frequency	alpha	48
	beta	48
	gamma	48
condition	active	48
	passive	48
	rest	48

Tests of Between-Subjects Effects

Dependent Variable:Mean Power

Source	Type III Sum of Squares	df	Mean Square	F	Sig.
Corrected Model	7753.663[a]	8	969.208	7.802	.000
Intercept	10253.818	1	10253.818	82.542	.000
frequency	6802.333	2	3401.166	27.379	.000
condition	512.426	2	256.213	2.062	.131
frequency * condition	438.904	4	109.726	.883	.476
Error	16770.367	135	124.225		
Total	34777.847	144			
Corrected Total	24524.029	143			

Estimated Marginal Means of Mean Power

SUMMARY:

The PMA *did not* have a significant interaction (p=.476) between frequency and condition despite the interaction when all 4 brain areas were combined (M1, SMA, PMA, S1.) When further simple effects were computed for each frequency band, there was still no significance:

Alpha - p = .277
Beta - p = .412
Gamma - p = .476

See following page for Simple Effect outputs.

see previous page for explanation

Tests of Between-Subjects Effects

Dependent Variable:Mean Power

		Source	Type III Sum of Squares	df	Mean Square	F	Sig.
Alpha Simple Effects		Corrected Model	880.208[a]	2	440.104	1.321	.277
		Intercept	15009.403	1	15009.403	45.053	.000
		frequency	.000	0	.	.	.
		condition	880.208	2	440.104	1.321	.277
		frequency * condition	.000	0	.	.	.
		Error	14991.732	45	333.150		
		Total	30881.343	48			
		Corrected Total	15871.940	47			

Tests of Between-Subjects Effects

Dependent Variable:Mean Power

		Source	Type III Sum of Squares	df	Mean Square	F	Sig.
Beta Simple Effects		Corrected Model	68.853[a]	2	34.426	.905	.412
		Intercept	1975.726	1	1975.726	51.964	.000
		frequency	.000	0	.	.	.
		condition	68.853	2	34.426	.905	.412
		frequency * condition	.000	0	.	.	.
		Error	1710.948	45	38.021		
		Total	3755.528	48			
		Corrected Total	1779.801	47			

ests of Between-Subjects Effects

Dependent Variable:Mean Power

		Source	Type III Sum of Squares	df	Mean Square	F	Sig.
Gamma Simple Effects		Corrected Model	2.269[a]	2	1.135	.754	.476
		Intercept	71.021	1	71.021	47.218	.000
		frequency	.000	0	.	.	.
		condition	2.269	2	1.135	.754	.476
		frequency * condition	.000	0	.	.	.
		Error	67.686	45	1.504		
		Total	140.976	48			
		Corrected Total	69.955	47			

APPENDIX B.2 – SPSS Output for Symmetry index Data (Result Section 3.2)

Univariate 3-way ANOVA
Dependent Variable: Symmetry index
Fixed Factors: Condition, Hemisphere
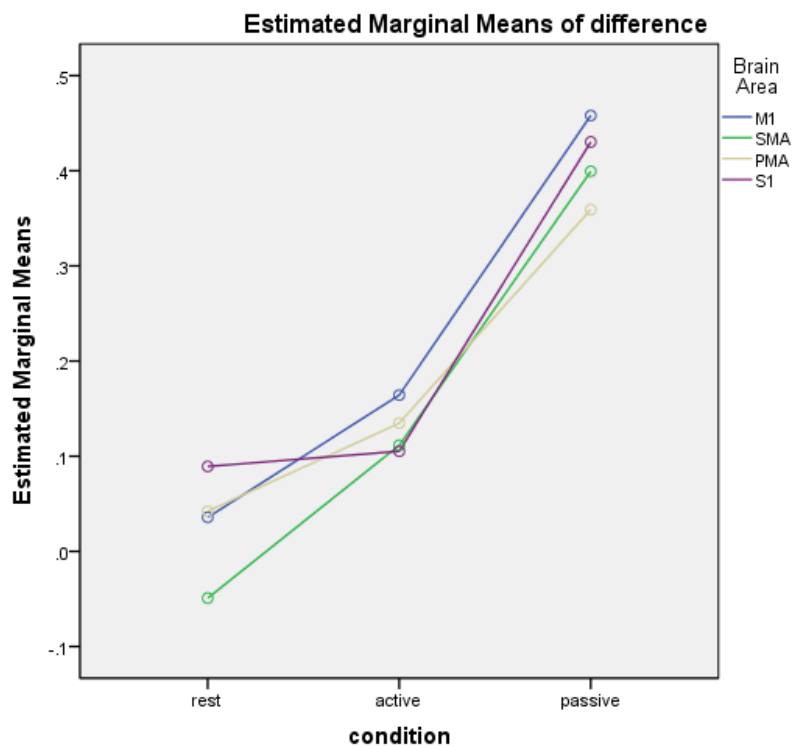Random Factors: Subject, Brain Area

Between-Subjects Factors

		Value Label	N
condition	1	rest	64
	2	active	64
	3	passive	64
hemisphere	1	left	96
	2	right	96
Brain Area	1	M1	48
	2	SMA	48
	3	PMA	48
	4	S1	48
subject	1		24
	2		24
	3		24
	4		24
	5		24
	6		24
	7		24
	8		24

Tests of Between-Subjects Effects

Dependent Variable:difference

Source		Type III Sum of Squares	df	Mean Square	F	Sig.
Intercept	Hypothesis	6.936	1	6.936	6.851	.040
	Error	5.968	5.895	1.012[a]		
condition	Hypothesis	5.034	2	2.517	7.691	.011
	Error	2.971	9.077	.327[b]		
hemisphere	Hypothesis	3.312	1	3.312	2.686	.151
	Error	7.600	6.165	1.233[c]		
BrainArea	Hypothesis	.126	3	.042	1.739	.749
	Error	.005	.217	.024[d]		
subject	Hypothesis	7.692	7	1.099	1.358	.487
	Error	1.622	2.004	.809[e]		
condition * hemisphere	Hypothesis	.295	2	.148	.160	.854
	Error	11.428	12.401	.922[f]		

condition * BrainArea	Hypothesis	.154	6	.026	.513	.778
	Error	.086	1.726	.050[g]		
condition * subject	Hypothesis	5.607	14	.401	.422	.939
	Error	12.568	13.254	.948[h]		
hemisphere * BrainArea	Hypothesis	.013	3	.004	.126	.932
	Error	.029	.811	.036[i]		
hemisphere * subject	Hypothesis	9.190	7	1.313	1.406	.283
	Error	11.982	12.832	.934[j]		
BrainArea * subject	Hypothesis	2.697	21	.128	2.063	.245
	Error	.262	4.210	.062[k]		
condition * hemisphere * BrainArea	Hypothesis	.433	6	.072	.596	.732
	Error	5.084	42	.121[l]		
condition * hemisphere * subject	Hypothesis	13.586	14	.970	8.016	.000
	Error	5.084	42	.121[l]		
condition * BrainArea * subject	Hypothesis	4.154	42	.099	.817	.742
	Error	5.084	42	.121[l]		
hemisphere * BrainArea * subject	Hypothesis	1.773	21	.	.	.
	Error	.	.	.[m]		
condition * hemisphere * BrainArea * subject	Hypothesis	5.084	42	.121	.	.
	Error	.000	0	.[n]		

Estimated Marginal Means of difference

SUMMARY:
From the 3-way ANOVA, we see that there is a significant global condition effect (p=.011). Also, there is no significant effect of Hemisphere or Subject (p=.151, p=.487), so we are able to combine all those variables to get the resulting figure (to the left).

2-way ANOVA – collapsed over Brain Area

Between-Subjects Factors

		Value Label	N
condition	1	rest	64
	2	active	64
	3	passive	64
hemisphere	1	left	96
	2	right	96

Tests of Between-Subjects Effects

Dependent Variable:difference

Source	Type III Sum of Squares	df	Mean Square	F	Sig.
Corrected Model	8.642^a	5	1.728	6.365	.000
Intercept	6.936	1	6.936	25.542	.000
condition	5.034	2	2.517	9.269	.000
hemisphere	3.312	1	3.312	12.197	.001
condition * hemisphere	.295	2	.148	.544	.581
Error	50.509	186	.272		
Total	66.086	192			
Corrected Total	59.151	191			

Multiple Comparisons

difference

Tukey HSD

(I) condition	(J) condition	Mean Difference (I-J)	Std. Error	Sig.	95% Confidence Interval	
					Lower Bound	Upper Bound
rest	active	-.099	.092	.528	-.317	.118
	passive	-.382[*]	.092	.000	-.600	-.165
active	rest	.099	.092	.528	-.118	.317
	passive	-.283[*]	.092	.007	-.500	-.065
passive	rest	.382[*]	.092	.000	.165	.600
	active	.283[*]	.092	.007	.065	.500

Based on observed means.

 The error term is Mean Square(Error) = .272.

*. The mean difference is significant at the 0.05 level.

1-way ANOVA – condition

Between-Subjects Factors

		Value Label	N
condition	1	rest	64
	2	active	64
	3	passive	64

Tests of Between-Subjects Effects

Dependent Variable:difference

Source	Type III Sum of Squares	df	Mean Square	F	Sig.
Corrected Model	5.034[a]	2	2.517	8.791	.000
Intercept	6.936	1	6.936	24.223	.000
condition	5.034	2	2.517	8.791	.000
Error	54.116	189	.286		
Total	66.086	192			
Corrected Total	59.151	191			

Multiple Comparisons

Tukey HSD

(I) condition	(J) condition	Mean Difference (I-J)	Std. Error	Sig.	95% Confidence Interval	
					Lower Bound	Upper Bound
rest	active	-.09942415720910	.094592818131183	.546	-.32288326013839	.12403494572019
	passive	-.38224267690163*	.094592818131183	.000	-.60570177983092	-.15878357397234
active	rest	.09942415720910	.094592818131183	.546	-.12403494572019	.32288326013839
	passive	-.28281851969252*	.094592818131183	.009	-.50627762262181	-.05935941676323
passive	rest	.38224267690163*	.094592818131183	.000	.15878357397234	.60570177983092
	active	.28281851969252*	.094592818131183	.009	.05935941676323	.50627762262181

T-test: Rest vs. Zero – *not significant*

One-Sample Statistics

	N	Mean	Std. Deviation	Std. Error Mean
difference	64	.029	.421	.052

One-Sample Test

	Test Value = 0					
					95% Confidence Interval of the Difference	
	t	df	Sig. (2-tailed)	Mean Difference	Lower	Upper
difference	.560	63	.577	.0295	-.075	.134

T-test: Rest LH vs. RH – *not significant between hemispheres*

Group Statistics

	hemisphere	N	Mean	Std. Deviation	Std. Error Mean
difference	left	32	.109	.353	.062
	right	32	-.050	.471	.083

Independent Samples Test

	Levene's Test for Equality of Variances		t-test for Equality of Means		
	F	Sig.	t	df	Sig. (2-tailed)
diff Eq var assumed	1.293	.260	1.526	62	.132
Eq var not assumed			1.526	57.435	.132

T-test: active LH vs. RH – *not significant between hemispheres*

Group Statistics

	hemisphere	N	Mean	Std. Deviation	Std. Error Mean
difference	left	32	.269	.470	.083
	right	32	-.0112	.653	.115

Independent Samples Test

		Levene's Test for Equality of Var		t-test for Equality of Means		
		F	Sig.	t	df	Sig. (2-tailed)
diff	Equal var assumed	1.399	.241	1.968	62	.054
	Equal var not assumed			1.968	56.339	.054

T-test: passive LH vs. RH – *significant difference between hemispheres*

Group Statistics

	hemisphere	N	Mean	Std. Deviation	Std. Error Mean
difference	left	32	.586	.346	.061
	right	32	.237	.717	.127

Independent Samples Test

		Levene's Test for Equality of Variances		t-test for Equality of Means		
		F	Sig.	t	df	Sig. (2-tailed)
difference	Equal variances assumed	19.778	.000	2.479	62	.016
	Equal variances not assumed			2.479	44.691	.017

APPENDIX C – Experiment Protocol Sheet

Pedaling in the MEG Experiment Sheet

Subject_____

<u>**Setup**</u>   Date_____

sensor/electrode	channel	plug location
EMG on R/L ____	EMG062	████████
EMG on R/L ____	EMG063	████████
Encoder Position	MISC001	Outlet 1
Encoder Speed	MISC002	Outlet 2
ECG	ECG064	████████
EOG	EOG061	████████
R Finger Tapper	STI101	Outlet 15
L Finger Tapper	STI101	Outlet 16
R Foot Tapper	STI101	Outlet 2
L Foot Tapper	STI101	Outlet 3

*possible EMG location
    -VM for pedaling
    -RF for pedaling

*explain all tests to subject-
 instructions on following pg.

Input into MEG GUI:
   ____ **Project:** Pedaling
   ____ **File → Load Settings →** Choose 'Experiment'
   ____ **Gantry position:** Supine

Subject is **right / left** handed according to Edinburgh Handedness Test.

**********zero encoder**********
<u>**Protocol**</u>
-remind subject to keep eyes open throughout whole experiment & stay relaxed

Run	Test	Raw file name	Length
01	Empty Room	run01_emptyroom_raw	2 min
02	Spontaneous Eyes Open	run02_spontaneous_raw	2 min
03	Continuous Finger Tapping	run03_finger_raw	~4 min
04	Cont. Alternating Finger Tapping	run04_altfinger_raw	2 min
05	Continuous Foot Tapping	run05_foot_raw	~4 min
06	Cont. Alternating Foot Tapping	run06_altfoot_raw	2 min
07	Continuous Active Pedaling	run07_active_raw	2 min
08	Continuous Active Pedaling	run08_active_raw	2 min
09	Block Pedaling	run09_blockpedal_raw	2 min
10	Block Pedaling	run10_blockpedal_raw	2 min
11	Continuous Passive Pedaling*	run11_passive_raw	2 min
12	Continuous Passive Pedaling*	run12_passive_raw	2 min
13	Increasing Velocity Pedaling	run13_incvelocity_raw	2 min
14	Pace Change Block Pedaling*	run14_pace_raw	3 min
15	Pace Change Block Pedaling*	run15_pace_raw	3 min

* uses auditory cue

<u>**Notes**</u>

<u>Instructions for the tests:</u>

Continuous finger and foot tapping consists of 30 second bouts of tapping, i.e. 30s R, 30s L, 30sR, 30s L, 30s R, 30s L. I will cue you as to when to start and stop each bout and which leg it will be. All tapping should be at a constant, comfortable pace. When not tapping, keep the finger or foot resting on the pad.

Ask to see them tapping after set-up

Continuous alternating finger and foot tapping will consist of 2 minutes of alternating RLRLRLRL, etc. tapping. The tapping should be at a constant, comfortable pace.

Ask to see them tapping after set-up

Active pedaling requires the subject to pedal for 2 minutes at a constant, comfortable self-chosen pace.

Make sure it is not fast enough to cause head movement

Block pedaling will have the subject pedaling for several second bouts. The pace should approximately be the same as the active pedaling rate. Subject may start and stop as they wish. Do not count the amount of time you are pedaling and the amount of time you are resting.

Passive pedaling will require an experimenter to pedal the bike while the subjects' feet are secured in the pedals. The experimenter receives an auditory cue as to how fast the pedaling pace should be. The subject should be *completely* relaxing their leg muscles and should not be exerting any force.

Increasing velocity pedaling will consist of a 2 minute scan with the subject starting at a "slow" self-pace and then gradually increase their speed. The end speed should be medium-fast, making sure that the head is not moving back and forth.

Explain that the increase is over 2 minutes and not to be done all at once

Pace change block pedaling will be 3-1 minute bouts of constant pedaling at a slow, medium and fast pace. These paces will be given in an auditory cue to the subject to test and then taken away for the 1 minute of recording for each pace.